

THE FORMATION OF CINNABAR-METACINNABAR AT HIDROTHERMAL CONDITIONS (BETWEEN 25°–300°C TEMPERATURE) AND ITS GENETICAL INTERPRETATION

J. KISS

Department of Mineralogy, Eötvös University, Budapest

and

A. ABDEL REHIM

Alexandria University

Received: 15 October 1976

Summary

Observations on natural mercury mineralizations provide controversial data about the formation α - β mercury sulfides (cinnabar-metacinnabar) as both modifications can exist in same genetical type of mineralization, which is characterised by enantiotropic temperature range. Both cubic (metacinnabar) and trigonal (cinnabar) have been recorded as first precipitations.

During the laboratory experiments systems HgCl_2 - H_2S - H_2O and HgNO_3 - H_2S - H_2O have been studied in temperature range between 25°–100 °C. Structural and morphological deformations of cubic modification formed on 25 °C have been investigated in temperatures between 50°–300 °C.

The role of As, Sb, Tl trace elements in the formation of cinnabar-metacinnabar have also been studied.

These chemical, crystal-chemical investigations provide additional data to the genetic interpretation of mercury deposits.

Introduction

Mercury deposits have generally simple mineralogical composition, mainly consisting of HgS - Hg - Sb_2S_3 and few other associated elements. The deposits are characterised by the dominance of *S*, *Ca*, *Si* (*Fe*, *Mg*) and *O* elements, *As*, *Sb* and *Cu* chalcophile elements, occasional concentrations of *Au*, *Ag*, *Bi*, *Pb*, *Zn*.

The average concentration of mercury in the Earth's crust is 0, 0X ppm:

Vinogradov	(1949, 1963)	= 0,07–0,083 ppm
Taylor	(1964)	= 0,08 ppm

The concentration is not affected by the acidity of igneous rocks (Turekian – Wedepohl, 1961, Vinogradov, 1962 third column; Ehmann – Lovering 1967):

ultrabasites	= 0,01–0,0X	ppm (4 ppb)
basic	= 0,09	ppm (7 ppb)
intermediate (syenite)	= 0,0X	ppm (4 ppb)
acid (granite)	= 0,08	ppm (39 ppb)

During the late crystallization phases, the amount of Hg in pegmatites less than 0,0X ppm, increasing in kata- and mesothermalites and reaches its peak at epithermal conditions. Volcanic exhalations generally have significant mercury content.

The Hg concentrations in sedimentary environment:

a) shales	0,40 ppm
b) sandstones	0,03 ppm
c) carbonates	0,04 — 0,0X ppm
d) pelites	0,X ppm

Usually high Hg concentration is recorded in the air above mercury deposits. This fact is used as exploration tool. Organisms (algae, fishes) show few tenths of $\mu\text{g}/\text{kg}$ Hg content.

The most important minerals of mercury are the α - β - γ -HgS, cinnabar and metacinnabar and the native mercury. Schwazite (HgS up to 24 per cent Hg), livingstonite ($(\text{HgSb}_4\text{S}_8)$), montroydite (HgO), guadalcazarite ($\text{HgZn}(\text{S}, \text{Se})$), onophrite ($\text{Hg}(\text{S}, \text{Se})$), coloradite (HgTe), tiemannite (HgSe), kleinite $\text{Hg}_2\text{N}(\text{Cl}, \text{SO}_4) \cdot n\text{H}_2\text{O}$, mosesite ($\text{Hg}_2\text{NCl} \cdot \text{H}_2\text{O}$), terlinguaite ($2\text{HgO} \cdot \text{Hg}_2\text{Cl}_2$), eglestonite ($\text{Hg}_6\text{Cl}_4\text{O}$) are rare accessories in mercury deposits. The oxide-chlorides are possible products of the vapor phase.

There are several opinions about the formation of cinnabar-metacinnabar:

- metacinnabar crystallises prior to cinnabar (αHgS)
- metacinnabar and cinnabar are crystallising syngenetically
- formation of metacinnabar follows that of αHgS
- metacinnabar precipitates from solutions and is not an alteration product of cinnabar
- metacinnabar has supergene origin.

In hot brines of Amadee Hot Spring, California, and Bouiling Spring, Idaho, metacinnabar (βHgS) crystallises, subsequent to cinnabar. There are examples for reversed precipitation sequences too. The formation of metacinnabar is probably affected by temperature, and probably, the pH conditions and the chemical assemblage, however the effects of the latter factor has not been experimentally proved yet. Near the mouth of Amadee Hot Spring precipitations, of cinnabar, metacinnabar, in outer zones drops of native mercury has been observed from the alkaline hot brines. From hot brines at Sulphur Bank California, similar phenomena have been recorded.

At Bouiling Spring (Valley County, Idaho) crystallisation of Mn-rich metacinnabar have been described, at 7–8 m distance from the mouth of the Spring. Cinnabar has formed near the mouth, associated with calomel, Hg-oxide-chloride, chalcedony, quartz, montmorillonite, alunite.

K r a u s k o p f (1951) has suggested a temperature range $80^{\circ} - 250^{\circ} \text{C}$ at 30 at pressure for the formation of cinnabar. D i c k s o n (1964) has given $100 - 230^{\circ} \text{C}$ temperature at 30 at pressure. The solubility of HgS in Na_2S solution had first studied by K n o x (1906), then D i c k s o n (1964), W h i t e et al (1967) at $3.5 - 7.5$ pH, $25^{\circ} - 200^{\circ} \text{C}$ temperatures, $4 - 140$ at pressures.

Based on conclusions about the $\text{HgS} - \text{H}_2\text{O} - \text{Na}_2\text{S}$ system, it seems that alkalinity has favourable effect on the formation of HgS. The $(\text{SO}_4)^{2-}$ content of alkaline hot brines (Na_2SO_4) indicates that Na_2S has an important role in solubility and transport of HgS. Based on



$$K \text{ is equal to } \frac{\text{Na}_2\text{HgS}_2}{(\text{Na}_2\text{S})\text{HgS}}$$

hence Na_2S increases the solubility of HgS. With increasing temperature the solubility of silicates (e. g. quartz) is also increasing. This gives an explanation for the relationship of HgS mineralization and siliceous environment. The coefficients of solubility:

Cinnabar $K = 10^{-3.50} (10^{-3.51})$ (S c h w a r z e n b a c h - W i d m e r)
 Metacinnabar $K = 10^{-5.9} (10^{-3.60})$ (S c h w a r z e n b a c h - W i d m e r)
 The solubility of HgS in the $\text{HgS}_{(s)} - \text{Na}_2\text{S}_{(aq)}$ system is increasing from 20°C to 100°C , decreasing between $100^{\circ} - 150^{\circ} \text{C}$, then gradually increasing. At room temperature the solubility of metacinnabar is 30 per cent larger than that of cinnabar. Until the inversion temperature for metacinnabar-cinnabar (344°C) is not reached 30 per cent of the crystalline phase is cinnabar.

The irreversibility of $\text{HgS}_{(s)} + \text{Na}_2\text{S}_{(aq)} \rightleftharpoons \text{Na}_2\text{HgS}_2$ system is highly influenced by the CO_2 content and oxygen saturation of the solution. This phenomenon plays important role in the formation of HgS and mercury deposits in carbonate environment (Algeria, New Idria - USA, R ó k a h e g y - Hungary)

In the $\text{HgS}_{(s)} + 2\text{H}_2\text{S}_{(aq)} \rightleftharpoons \text{HgS}(\text{H}_2\text{S})_{2(aq)}$ system at 20°C temperature

$$\begin{array}{ll} K = 10^{-4.25} & \text{cinnabar} \\ K = 10^{-4.31} & \text{metacinnabar} \end{array}$$

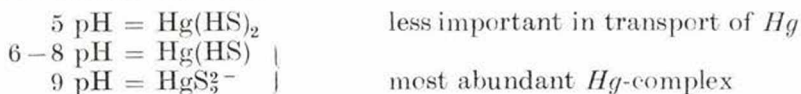
In the $\text{HgS} + \text{S}^{2-} = \text{HgS}_2^{2-}$ system B a r n e s (1976) suggested

$$\begin{array}{l} K = 10^{+0.57} = \text{metacinnabar} \\ K = 10^{+0.48} = \text{cinnabar} \end{array}$$

These data indicate that formation of deposits composed of Hg - HgS are associated by alkaline + HgS_2^{2-} - hydrothermal solutions.

D r e y e r (1940) concluded that most HgS deposits form at near-surface conditions, on normal pressure. D i c k s o n (1964) stated that HgS mineralizations could form at low pressure (1 - 30 at) and temperature

100°–230 °C from neutral — or slightly alkaline solutions, because stability ranges of Hg-complexes are determined by the above-mentioned physico-chemical parameters.



In sulfide-complexes mercury is linked to chains with 2 or 4 coordination, these govern the development of chain structures of cinnabar or framework structure of metacinnabar (Barnes et al. 1967. Fig. 1).

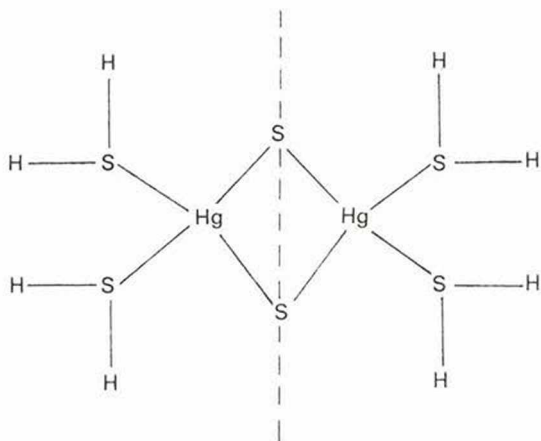
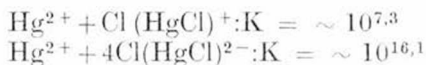


Fig. 1. Co-ordinating ligands of the HgS (Barnes et al.)

As indicated by several Hg-chloride minerals, transfer of mercury in chloride-complexes is also a possibility. The stability of Hg-chlorides is strongly temperature dependent, these minerals occur rarely compared to the HgS modifications, (Krauskopf 1951).

The equilibrium constants of Hg-chloride complexes:



Hydrothermal experiments

Laboratory experiments have been carried out in liquid-vapor and solid-liquid phase systems:

a) Synthesis of HgS monophasic from solutions containing Hg⁺ and Hg²⁺ ions at 25°–50°–75°–100°C temperatures

1. (0.1 mol HgNO_{3(aq)} + H₂S_(g))
2. 0.1 mol HgCl_{2(aq)} + H₂S_(g))

b) Effects of As^{3+} , Sb^{3+} , Tl^+ on the formation of HgS (by $\text{Hg}:\text{R}$ ratios of 100:1 and 1000:1):

1. 0,1 mol $\text{HgCl}_{2(aq)} + \text{AsCl}_3 + \text{H}_2\text{S}_{(g)}$
2. 0.1 mol $\text{HgCl}_{2(aq)} + \text{SbCl}_3 + \text{H}_2\text{S}_{(g)}$
3. 0.1 mol $\text{HgCl}_{2(aq)} + \text{TlCl} + \text{H}_2\text{S}_{(g)}$

As, *Sb*, *Tl* have been chosen as "impurities", because the stabilities of their sulfide-complexes are similar to that of HgS , atomic radii are near to that of *Hg*, and occur in epithermal ore deposit.

c) HgS ($=\beta\text{HgS}$ -metacinnabar) + H_2O and $\beta\text{HgS}_{(aq)} + \text{Na}_2\text{S}_{(g)}$ systems between 25₂–300 °C. HgS is synthesised from $\text{HgCl}_{2(s)} + \text{H}_2\text{S}_{(aq)}$ system at 25 °C.

d) Metacinnabar (βHgS) in solutions with composition $\text{Hg}:\text{R} = 100:1$ between 50°–300 °C. ($\text{R} = \text{As}^{3+}$, Sb^{3+} , Tl^+).

Laboratory experiments are calculated with mercury ions migrating in chloride-complexes, from which HgS phases can be formed irreversibly by the effect of H_2S – Na_2S hydrothermal solutions.

Hg -ions in nitrate complexes have been investigated to study the effect of synchronous or differentiated formation of α - and βHgS .

1) 0.1 mol $\text{HgNO}_{3(aq)} - \text{H}_2\text{S}_{(g)}$ system

The experiments have been carried out from 0.1 mol mercury (I) nitrate solution with initial pH 2.3. The pH value of the solution have been modified during the reactions:

25 °C	15 min	1.00 pH metacinnabar crystallites
	60 min	0.84 pH metacinnabar crystallites
	8 hours	0.85 pH cinnabar
	20 hours	0.85 pH cinnabar
	30 hours	0.85 pH cinnabar
50 °C	60 min	0.85 pH cinnabar
	8 hours	0.85 pH cinnabar + Hg-drops
65 °C	8 hours	1.19 pH $\beta\text{HgS} > \alpha\text{HgS}$
75 °C	60 min	1.05 pH βHgS crystallites
	4 hours	1.06 pH βHgS crystallites
	8 hours	1.21 pH $\beta\text{HgS} - \alpha\text{HgS}$?
	12 hours	1.19 pH βHgS
100 °C	10 min	1.01 pH –
	60 min	1.00 pH βHgS crystallites
	8 hours	(?) 1.0 pH $\beta\text{HgS} > \alpha\text{HgS}$

* The use of mercury (I)-nitrate is supported by two factors:

a) very low solubility of Hg_2Cl_2 ,

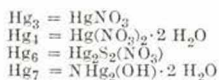
b) anion effects on the formation of HgS modifications.

These data indicate that acidity of solutions formed within the same time-intervals (8 hours) is larger for αHgS (pH 0.85) than for βHgS and $\beta\text{HgS} > \alpha\text{HgS}$ (1.08–1.21 pH). Different time intervals (15 min–30 hours) have been used for observations of transitional and accessory phases during the experiments. It was found that formation of stable sulphide phases is preceded by multi-phase precipitation of white or greyish-white Hg-compounds: $(\text{HgNO}_3 \cdot 2\text{H}_2\text{O}; \text{NHg}_2\text{OH} \cdot 2\text{H}_2\text{O}$ and $\text{NHg}_2(\text{NO}_3)$. The advance of the process is marked by the increasing, appearance of black and brownish-red precipitation of HgS (Table I.)

Table I.

Crystalline phases of the $\text{HgNO}_{3(aq)} - \text{H}_2\text{S}_{(g)}$ -system

Temperature	Time	Colour of reaction product	Crystalline phases
25°C	15 min.	dark gray	βHgS crystallites + $\text{Hg}_3, \text{Hg}_4, \text{Hg}_6, \text{Hg}_7$
25°C	60 min.	black	$\beta\text{HgS} + \text{Hg}_4$
25°C	8 hours	reddish-brown	$\alpha\text{HgS} + \text{metallic Hg drops}$
25°C	20 hours	brown	$\alpha\text{HgS} + \text{Hg} + \text{,,}$
25°C	30 hours	reddish-brown	$\alpha\text{HgS} + \text{,,}$
50°C	60 min.	black and gray	$\alpha\text{HgS}, \text{Hg}_4$
50°C	8 hours	brown reddish brown	$\alpha\text{HgS} + (-)$
65°C	8 hours	dark-gray	$\beta\text{HgS} \gg \alpha\text{HgS} + \text{Hg} + \text{Hg}_3\text{S}_2(\text{NO}_3) ?$
75°C	60 min.	black lamellae, gray	$\beta\text{HgS} + \text{Hg}_3, \text{Hg}_4$
75°C	4 hours	gray	$\beta\text{HgS} + \text{Hg}_3, \text{Hg}_4, \text{Hg}_3\text{S}_2(\text{NO}_3)$
75°C	8 hours	gray, grayish white	$\beta\text{HgS}, \alpha - \text{HgS} (?) + \text{HgNO}_3, \text{Hg}_4$
75°C	10 hours	black and gray	$\beta\text{HgS} + \text{Hg}_3, \text{Hg}_4$
75°C	12 hours	black	$\beta\text{HgS} \gg \alpha\text{HgS} + \text{Hg}_4$
100°C	60 min.	gray, black	βHgS crystallites + $\text{Hg}_3, \text{Hg}_4, \text{Hg}_7$
100°C	8 hours	black, pale gray	$\beta\text{HgS} \gg \alpha\text{HgS} + \text{Hg}_3 + \text{Hg}_4 + \text{Hg}_7$



In the $\text{Hg}(\text{NO}_3)_{(aq)} - \text{H}_2\text{S}$ system the cubic βHgS had been formed first at all temperatures, along with $\text{HgNO}_3, \text{HgNO}_3 \cdot 2\text{H}_2\text{O}, \text{Hg}(\text{NO}_3)_2 \cdot 2\text{H}_2\text{O}$ and possibly $\text{Hg}_2\text{S}_2(\text{NO}_3)$. Following the formation of $\text{Hg}_2\text{S}_2(\text{NO}_3)$ the HgNO_3 bonds can split, $\text{Hg}(\text{HS}), \text{Hg}(\text{HS})_2, \text{HgS}_2^{2-}$ complexes and finally the poorly soluble HgS can form. No other final phases exist beside cinnabar (αHgS). The solution exhibits the greatest acidity (0.85 pH).

Pure HgS phases have been obtained at 25°–50 °C temperature, 8 hours. At 75 °C in different time intervals (4–8 hours) both βHgS and $\alpha\text{HgS} + ?$ had been formed, therefore experiments have been repeated at 65 °C (8 hours) to obtain more exact data about $\beta\text{HgS} \rightleftharpoons \alpha\text{HgS}$ reaction. These experiments indicated that in the $\text{HgNO}_3 + \text{H}_2\text{S}$ system the temperature interval for contemporaneous formation of βHgS and αHgS is 50°–65 °C:



The sulphur-content of the crystalline phases in the $\text{HgNO}_3\text{-H}_2\text{S}$ system is highly variable due to formation of mercury:

25 °C/8 hours	= + 0.91% Hg and - 5.65% S
25 °C/20 hours	= + 3.28% Hg (Hg-drops have been separated) - 20.51% S(!)
50 °C/8 hours	= + 3.74% Hg (Hg-drops have been separated) - 30.44% S(!)

Stoichiometric ratios of HgS are shown in Table VI. Stoichiometric ratios (Hg:S) could not be determined precisely due to formation of metallic Hg and different Hg -nitrate complexes. ($\beta\text{HgS} > \alpha\text{HgS}$ phases formed during reactions at 65°–75°–100 °C/8 hours have not been analysed due to inadequate quantities of material obtained).

The c_0/a_0 cell parameters of αHgS formed at 25°–50 °C = 2.2891 – 2.2945 Å, at 75°–100° these values change to 2.3015 and 2.3064 Å respectively, indicating that the cell become more elongated. The $a_0 = 5.8682\text{--}5.8752$ Å of βHgS crystallites formed at 75 °C/60 min and 100 °C/60 min indicate less packed, while $a_0 = 5.8466\text{--}5.8597$ Å parameters obtained from experiments of 8–12 hours duration show tightly packed cells as compared indicating that the cell become more elongated. The $a_0 = 5.8682\text{--}5.8752$ Å of βHgS crystallites formed at 75 °C/60 min and 100 °C/60 min indicate (Table II and Fig. 2).

Table II

Chemical composition of the crystalline phases of the $\text{HgNO}_{3(aq)} + \text{H}_2\text{S}_{(g)}$ -system

T°	Hg	S
25°C	73,63 – 79,63%	11,02 – 9,74%
50°C	81,70 – 89,43%	9,77 – 9,60%
75°C	82,80 – 88,75%	5,83 – 7,73%
100°C	71,13 – 78,89%	6,88 – 10,21%

2) $\text{HgCl}_{2(aq)}\text{-H}_2\text{S}_{(gas)}$ system

The initial solution was 0.1 mol Hg (II) chloride with 4.1 pH, characterised by the following thermodynamical parameters:

$F^\circ = -42.2$ Kcal/mol	Robert (1971)
$F^\circ = -50.53$ Kcal/mol	Robert (1971)

In every case 500 ml solution have been used, reactions at 25°, 50°, 75°, 100 °C with durations of 8 hours- 45 min have been studied. During the experiments acidity have significantly decreased with time and temperature ($\text{pH} = 0.70\text{--}1.90$).

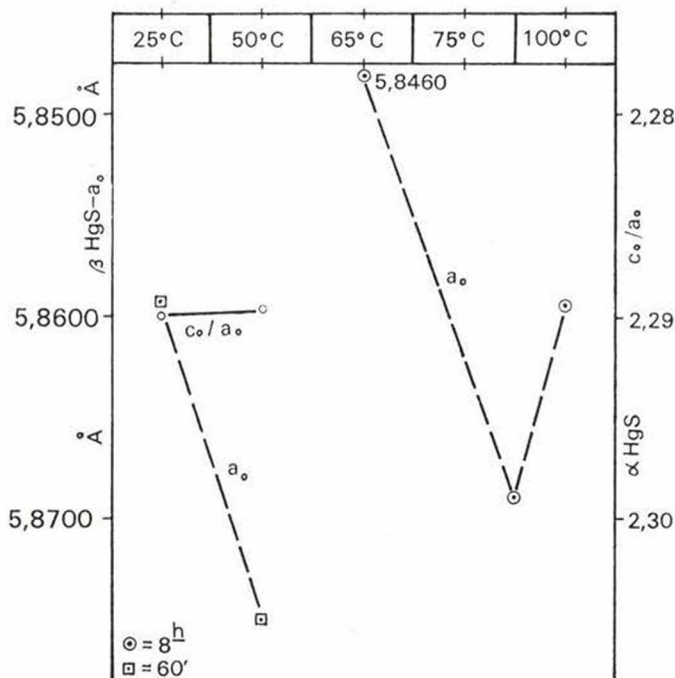


Fig. 2. $c_0/a_0 + a_0$ data of the crystalline phases of the $\text{HgNO}_{3(aq)} - \text{H}_2\text{S}$ -system.

25 °C	60 min	2.35 pH	
	95 min	1.75 pH	βHgS crystallites
	8 hours	0.84 pH	βHgS
50 °C	8 hours	0.82 pH	βHgS
75 °C	8 hours	0.80 pH	$\beta\text{HgS} \gg \alpha \text{HgS}$
100 °C	45 min	1.90 pH	
100 °C	8 hours	0.70 pH	$\beta\text{HgS} \gg \alpha \text{HgS}$

During the reaction precipitation of white colour ($\alpha - \gamma\text{HgS}_3\text{S}_2\text{Cl}_2$) have been formed first, followed by greyish and black products. At 25° - 50 °C metacinnabar, at 75° - 100° $\beta\text{HgS} + \alpha\text{HgS}$ phases (with βHgS dominance) precipitated, associated by the following accessories:

25 °C	60 min	gray	$\alpha - \beta\text{Hg}_3\text{S}_2\text{Cl}_2$
		greyish white	
25 °C	- 95 min	a) greenish-grey	βHgS crystallites and
		b) pale-grey	$\alpha - \gamma\text{Hg}_3\text{S}_2\text{Cl}_2$
		c) grey	
25 °C	8 hours	black	$\beta\text{HgS} + \gamma\text{Hg}_3\text{S}_2\text{Cl}_2$
50 °C	- 8 hours	black	$\beta\text{HgS} + \gamma\text{Hg}_3\text{S}_2\text{Cl}_2$
75 °C	- 8 hours	black	$\beta\text{HgS} + \alpha\text{HgS} +$ $\gamma\text{Hg}_3\text{S}_2\text{Cl}_2$

100 °C - 45 min	a) greenish grey b) pale-grey c) grey	$\alpha - \gamma \text{Hg}_3\text{S}_2\text{Cl}_2$
100 °C - 8 hours	black	$\beta > \alpha \text{HgS} + \text{Hg}_3\text{S}_2\text{Cl}_2$

The initial products of reactions in the $\text{HgCl}_{2(aq)} - \text{H}_2\text{S}_{(g)}$ system are the α - and $\gamma\text{Hg}_3\text{S}_2\text{Cl}_2$. From the two the modification has larger stability, however its presence in products of reactions at 75°–100 °C was not observed. Unlike in the $\text{Hg(I)-nitrate} - \text{H}_2\text{S}_{(g)}$ -system, βHgS with sphalerite-type structure has been formed at 25°–50°C temperature. At 57°–100 °C βHgS was the dominant product, but αHgS has also been recorded.

This indicates that in solution-vapour system the $\beta\text{HgS} \rightleftharpoons \alpha\text{HgS}$ reaction takes place between 50° and 65 °C. This has an implied explanation for controversial observations in natural systems, regarding the βHgS and αHgS precipitation sequence, (in several cases the black βHgS , in other cases the purple αHgS was recorded as first precipitation).

The formation of βHgS begins after the saturation of the solution with respect to sulphur has reached 60 per cent. Below this value of sulphur-saturation $\gamma\text{Hg}_3\text{S}_2\text{Cl}_2$ have been produced.

The chemical composition of crystalline phases of the $\text{HgCl}_{2(aq)} - \text{HgS}_{(g)}$ system (from experiments of 8 hours duration) are "richer" in Hg and S than the products of $\text{Hg(I)-nitrate} - \text{H}_2\text{S}_{(g)}$ -system (Table III. and Fig. 3).

The data obtained from the analyses indicate that the HgS formed in the $\text{Hg(II)-chloride} - \text{H}_2\text{S}$ system depleted in cations (Hg), but all the S-positions have been filled (?) (Table IV and VI).

Table III.

Chemical composition of the crystalline phases of the $\text{HgCl}_{2(aq)} - \text{H}_2\text{S}_{(g)}$ -system

T°	Hg	S	Cl	H ₂ O
25°C	85,84%	13,98%	0,26%	0,00%
50°C	84,79%	14,00%	0,15%	0,03%
75°C	85,04%	13,96%	0,41%	0,07%
100°C	84,56%	13,10%	2,19%	0,04%

The a_0 structural parameter of βHgS is decreasing with the rising temperature. The c_0/a_0 parameters of the αHgS have not been calculated, as only few $d/\text{Å}$ data have been obtained.

$$\begin{aligned}
 25^\circ/8\text{h} : a_0 &= 5.8610 \text{ \AA} \\
 50^\circ/8\text{h} : a_0 &= 5.8408 \text{ \AA} \\
 75^\circ/8\text{h} : a_0 &= 5.8011 \text{ \AA} \\
 100^\circ/8\text{h} : a_0 &= 5.7441 \text{ \AA}
 \end{aligned}$$

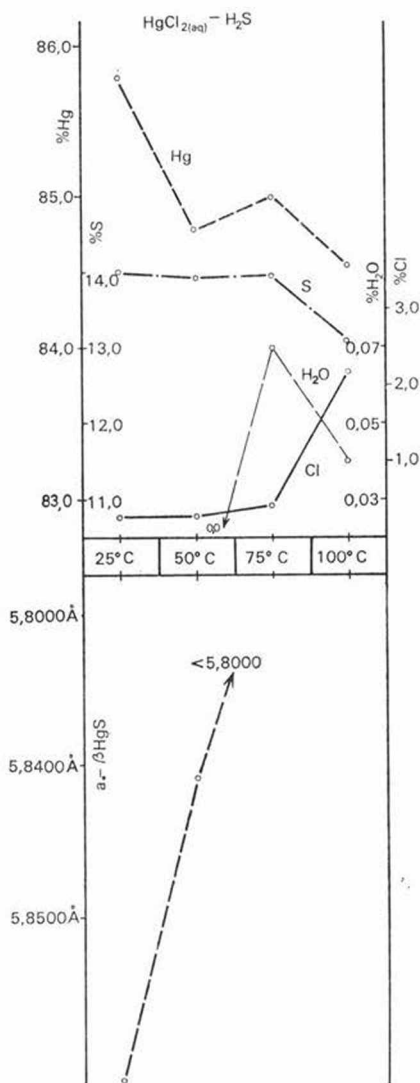


Fig. 3. Chemical composition of the crystalline phases of the $\text{HgCl}_{2(\text{s})} - \text{H}_2\text{S}_{(\text{g})}$ - system.

The decreasing cell-parameters of βHgS at 75°–100 °C can be related to the initial formation of αHgS structure.

Table IV.

The non stoichiometric composition of the $\text{HgS}_{(s)} + \text{H}_2\text{O}$; Na_2S ; R -chlorine systems

System	Hg					S				
	25°C	50°C	75°C	100°C		25°C	50°C	75°C	100°C	
$\text{HgNO}_{3(aq)} - \text{H}_2\text{S}$	-0,91	-3,74	-	-		-5,65	-30,44	-	-	
$\text{HgCl}_{2(aq)} - \text{H}_2\text{S}$	-0,42	-1,90	-1,35	-1,90		-1,30	-5,07	+1,16	-5,07	
100:1										
$\text{HgCl}_{2(aq)} - \text{AsCl}_{3(aq)} - \text{H}_2\text{S}$	-4,40	-3,27	-3,41	-1,36		+2,97	+3,55	+5,00	+5,29	
$\text{HgCl}_{2(aq)} - \text{SbCl}_{3(aq)} - \text{H}_2\text{S}$	-5,22	-4,34	-3,55	-3,47		-0,07	+10,58	+5,00	+10,94	
$\text{HgCl}_{2(aq)} - \text{TlCl} - \text{H}_2\text{S}$	-3,93	-3,74	-2,94	-3,25		+2,25	+2,97	+4,86	+2,97	
1000:1										
$\text{HgCl}_{2(aq)} - \text{AsCl}_3 - \text{H}_2\text{S}$	-0,28	-4,43	-4,47	-3,90		+1,23	+0,87	+1,74	+10,72	
$\text{HgCl}_{2(aq)} - \text{SbCl}_3 - \text{H}_2\text{S}$	-0,07	-1,76	-1,04	-4,19		+2,68	+0,29	+1,09	-0,29	
$\text{HgCl}_{2(aq)} - \text{TlCl} - \text{H}_2\text{S}$	-3,45	-4,44	-2,73	-4,30		+2,25	+2,39	+2,17	+3,19	

3. Experiments for recrystallization of βHgS formed at 25 °C in the temperature range between 25–350°C

3.1. $\text{HgS}_{(s)} - \text{H}_2\text{O}$

The structural inversion of βHgS , which was formed in Hg -chloride- H_2S system has characteristic features (posthydrothermal effect structural framework diagenesis).

The crystalline product, formed at 25°C/8 hours has the following composition:

Hg	= 85.79%
S	= 14.00%
Cl	= 0.26%
H ₂ O	= 0,00%
	100,05%

wich is equal to

βHgS	= 97.31%
$\text{Hg}_3\text{S}_2\text{Cl}_2$	= 2.69%
	100.00%

phase-composition. The compositional changes of this product in the 25°–300°C temperature range are shown in Fig. 4. (30 days at 25°C, 24 hours at 50°–300°C)

The Hg content is decreasing with an average 1.77 per cent, while the S content remains practically unchanged (+0.01%). The four Hg -“maximum” and three Hg -“minimum” varies with the temperature:

Hg -“maximum”	= a) 25°; b) 75°; c) 175°–200°; d) 350°C
Hg -“minimum”	= a) 50°; b) 100°–150°; c) 250°–300°C.

The Cl content is reducing with an average of 0.09 per cent, with the largest amount at 125°–150°C (=0,04%, 85 per cent of Cl content) and at 200°C. Approximately 40 per cent of total Cl content can be removed without any sign of destruction. The pH factor of the solution have been stabilized at 4.82–3.9 between 25°–75°C, above temperature it has become more acid at an average pH 2.24 (in the range of 2.10–2.37).

The inversion of βHgS to cinnabar starts at 25 °C/30 days. Between 25°–150°C the βHgS is still the dominant phase ($\beta\text{HgS} > \alpha\text{HgS}$), their proportion shows an opposite change between 175°–250°C, and only mono-phase αHgS have been observed at 300°–350° C (Fig. 5 and 6).

Using these results in the interpretation of mineral genesis it can be concluded the βHgS (metacinnabar) wich have initially crystallised from the hydrothermal solutions, can be altered to αHgS (cinnabar) at low temperatures by the effect of post-ore solutions. At higher temperatures the rate of inversion in increasing, and from 175°C the αHgS is the dominant crystal-phase. We dont have data about the rate of inversion below 175°C (It is possible that $\beta\text{HgS} \rightarrow \alpha\text{HgS}$ precipitations in eocene Nummulite-limestone at Rókahegy–Budapest can be explained with this processes).

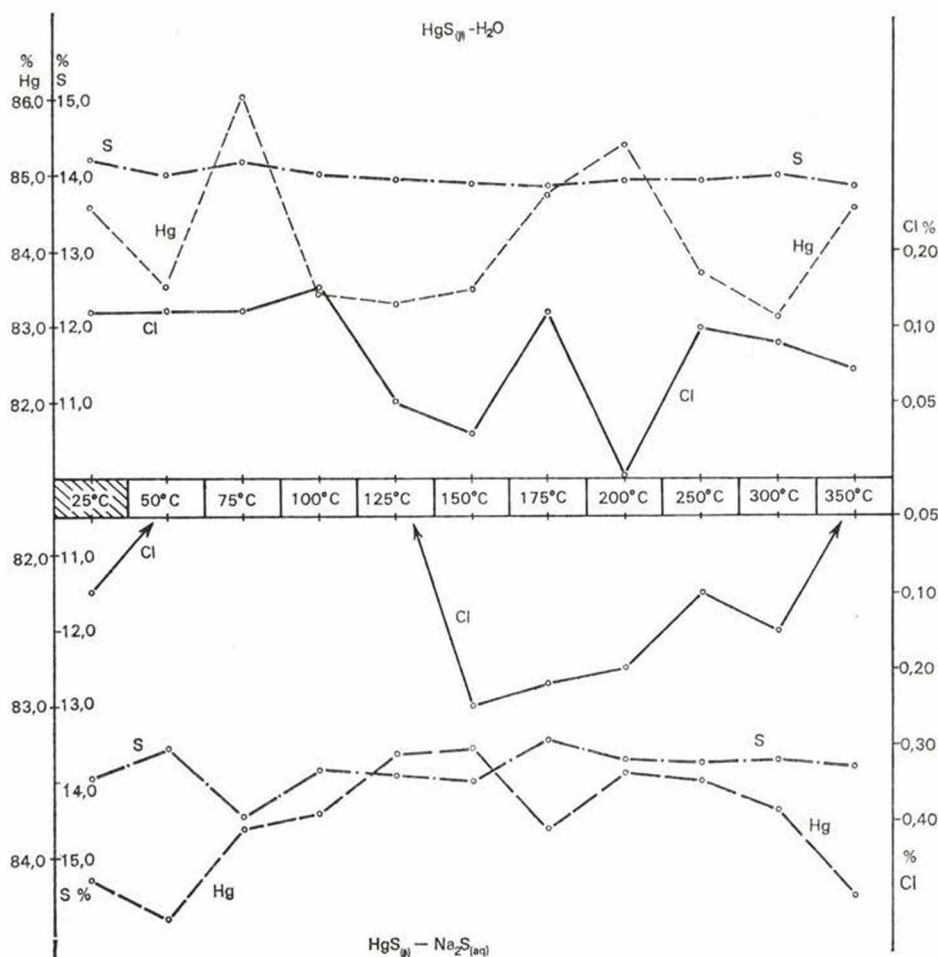


Fig. 4. The composition of $\text{HgS}_{(s)} + \text{H}_2\text{O}$ and $\text{HgS}_{(s)} + \text{Na}_2\text{S}_{(aq)}$ crystal phases as a function of T° .

SYSTEM	METACINNABAR (βHgS) - CINNABAR (αHg)										
	25°C	50°C	75°C	100°C	125°C	150°C	175°C	200°C	250°C	300°C	350°C
	β > >α	β > >α	β > >α	β > >α	β > >α	β > >α	α > >β	α > >β	α > >β	α	α
$\text{HgS}_{\beta} - \text{Na}_2\text{S}_{(aq)}$	β > >α	β > >α	α > >β	α	α	α	α	α	α	α	α
$\text{HgS}_{\beta} - \text{AsCl}_3_{(aq)}$	β	β	β	β	β	β	β > >α	α > >β	α > >β(?)	α	α
$\text{HgS}_{\beta} - \text{SbCl}_3_{(aq)}$	β	β > α (?)	β > α (?)	β	β > >α	β > >α	α > >β	α > >β	α	α	α
$\text{HgS}_{\beta} - \text{TlCl}_{(aq)}$	β	β	β	β	β	β > >α	β > >α	β > >α	α > >β	α	α

Fig. 5. Phase relations of $\text{HgS} + \text{solution}$ systems. The upper line refers to the $\text{HgS}_{(\beta)} - \text{H}_2\text{O}$ system

In the non-stoichiometric compositions of the $\beta\text{HgS} > \alpha\text{HgS}$ (at $25^\circ - 150^\circ\text{C}$), the $\alpha\text{HgS} > \beta\text{HgS}$ (at $175^\circ - 250^\circ\text{C}$) and αHgS ($300^\circ - 360^\circ\text{C}$) crystalline phases the following relationships have been observed (Table V and VI).

- a) $\beta\text{HgS} > \alpha\text{HgS} = -0.15 - 3.33\% \text{ Hg-deficiency and } +0.94 + 4.06\% \text{ S}$
 b) $\alpha\text{HgS} > \beta\text{HgS} = -0.89 - 2.88\% \text{ Hg-deficiency and } +0.65 + 1.16\% \text{ S}$
 c) $\alpha\text{HgS} = -1.88 - 3.52\% \text{ Hg-deficiency and } +5.58 + 1.52\% \text{ S}$

Mean values

- a) $\beta\text{HgS} > \alpha\text{HgS} = -2.46\% \text{ Hg} + 2.02\% \text{ S}$
 b) $\alpha\text{HgS} > \beta\text{HgS} = -2.37\% \text{ Hg} + 0.84\% \text{ S}$
 c) $\alpha\text{HgS} = -2.70\% \text{ Hg} + 1.05\% \text{ S}$

It seems that αHgS is no the average more deficient in cations than βHgS (However Barnes and Scott suggested the βHgS as *S*-deficient)

3.2. $\text{HgS}_{(s)} - \text{Na}_2\text{S}_{(aq)}$

Literature data show that the best solvent for HgS is the aqueous solution of Na_2S (Dickson 1964 Barnes - Romberger - Stemprow - 1967). Solubility is related to the concentration of Na_2S , at 250°C and 1800 bar has a value of 30 g/l. Phase-alterations has not been mentioned except that at temperatures below 344°C approximately 30% αHgS was formed.

The experiments in the $\text{HgS}_{(s)} - \text{Na}_2\text{S} - \text{H}_2\text{O}$ system have been initiated by the following problems:

- a) the saturation of *S*-deficient position can take place diagenetically
 b) if chlorine is removed the transitional reaction product, $\gamma\text{Hg}_3\text{S}_2\text{Cl}_3$ alters to HgS ,
 c) what is the alteration temperature of complete inversion of βHgS to αHgS ,
 d) How the cell-parameters are changing during the $\beta\text{HgS} \rightarrow \alpha\text{HgS}$ alterations.

0.1 mol Na_2S solution has been used for the experiments with the $\text{HgS}_{(s)} - \text{Na}_2\text{S} - \text{H}_2\text{O}$ system. Experiments have been carried out in Pyrex-phials, in closed system. (The duration of experiments was 30 days at 25°C , 24 hours at $50^\circ - 350^\circ\text{C}$).

The chemical composition of the initial $\beta\text{HgS}_{(s)}$ showed the following variations during the phase alterations at $25^\circ - 350^\circ\text{C}$ (average values):

$$\begin{aligned} 25^\circ - 50^\circ &= -1.51\% \text{ Hg}, & -0.22\% \text{ S} \\ 75^\circ - 300^\circ &= -2.23\% \text{ Hg}, & -0.15\% \text{ S} \\ 350^\circ &= -1.54\% \text{ Hg}, & -0.21\% \text{ S} \end{aligned}$$

The following Cl contents have been analysed:

$$\begin{aligned} 150^\circ - 200^\circ\text{C} &= 0.20 - 0.25\% \text{ Cl} \\ 25^\circ - 125^\circ\text{C} &= 0 - 0.10\% \text{ Cl} \\ 250^\circ - 350^\circ\text{C} &= 0 - 0.15\% \text{ Cl} \end{aligned}$$

The pH of the solution showed slightly decreasing tendency:

$$\begin{aligned} 25^\circ - 200^\circ\text{C} &= 9.86 - 10.35 \\ 250^\circ - 300^\circ\text{C} &= 9.58 - 8.24 \end{aligned}$$

The βHgS phase alterations in the $\text{HgS} - \text{Na}_2\text{S} - \text{H}_2\text{O}$ system indicate that $\text{Na}_2\text{S} + \text{H}_2\text{O}$ solution (post-ore hydrothermal solution) accelerates the formation of αHgS and at $100^\circ - 350^\circ$ exclusively mono-phase cinnabar structure is formed:

- $25^\circ - 50^\circ\text{C} = \text{black, } \beta\text{HgS} > \alpha\text{HgS} + \gamma\text{Hg}_3\text{S}_2\text{Cl}_2$
- $75^\circ\text{C} = \text{brownish-red } \alpha\text{HgS} > \beta\text{HgS} + \gamma\text{Hg}_3\text{S}_2\text{Cl}_2$
- $100^\circ - 175^\circ\text{C} = \text{purple } \alpha\text{HgS} + \text{NaHgCl}_3 \cdot 2\text{H}_2\text{O}$
- $200^\circ - 350^\circ\text{C} = \text{purple } \alpha\text{HgS} + \gamma\text{Hg}_3\text{S}_2\text{Cl}_2$

(Table V., VI. and Fig 4.)

The non-stoichiometric compositions of $\beta\text{HgS} > \alpha\text{HgS}$;
 $\alpha\text{HgS} > \beta\text{HgS}$ and αHgS :

$$\begin{aligned} 25^\circ - 50^\circ\text{C} &= \beta\text{HgS} > \alpha\text{HgS} = -2.09 - 2.35\% \text{ Hg, } 1.16 - 1.52\% \text{ S} \\ 75^\circ\text{C} &= \alpha\text{HgS} > \beta\text{HgS} = -1.53 - 2.23\% \text{ Hg, } -0.65 + 4.9\% \text{ S} \\ 100^\circ - 350^\circ\text{C} &= \alpha\text{HgS} = -2.26 - 3.40\% \text{ Hg, } -0.07 + 1.52\% \text{ S} \end{aligned}$$

Mean values:

$$\begin{aligned} 25^\circ - 50^\circ\text{C} &= \beta\text{HgS} > \alpha\text{HgS} = -2.22\% \text{ Hg} - 0.36\% \text{ S} \\ - 50^\circ\text{C} &= \beta\text{HgS} > \alpha\text{HgS} = -2.22\% \text{ Hg} - 0.36\% \text{ S} \\ 75^\circ\text{C} &= \alpha\text{HgS} > \beta\text{HgS} = -2.18\% \text{ Hg} + 2.56\% \text{ S}^* \\ 100^\circ - 350^\circ\text{C} &= \alpha\text{HgS} = -2.98\% \text{ Hg} - 0.80\% \text{ S} \end{aligned}$$

On the average αHgS shows larger Hg and smaller S deficiency than βHgS , the $\text{Hg}:\text{S}$ ratio of αHgS approximates the ideal 1:1 value better than that of βHgS . The cello parameter for βHgS $a_0 = 5.8521 \pm 0.0007 \text{ \AA}$, is unaffected by temperature changes. The c_0/a_0 value of αHgS differs from literature data (2.30 \AA) with -0.01 \AA (Fig. 6).

a) The results given by the experiments in the $\text{HgS}_{(s)} - \text{Na}_2\text{S}_{(aq)}$ system indicate that effects of H_2S solutions promote splitting of $[\text{HgS}_4]$ -tetrahedra of βHgS and their chain like linear rearrangement (cinnabar structure). It also causes the alteration of accessory $\gamma\text{Hg}_3\text{S}_2\text{Cl}_2$ phase to αHgS by removing Cl . The non-stoichiometric character of αHgS becomes smaller despite the number of unfilled S -positions being larger than of βHgS .

b) The initially formed less stable βHgS phase alters to cinnabar quite easily, therefore αHgS is more abundant in nature. Coexisting $\alpha - \beta$ HgS indicates meta-phase transitional stage, which can explain the controversial conclusions in previous studies about the phenomenon that both meta-cinnabar and cinnabar have been observed as first precipitation.

* From data of 8-24-30 hours experiments.

Table V.

The non stoichiometric composition of the HgS

System	$\pm \text{Hg}$ $\pm \text{S}$	25°C	50°C	75°C	100°C	125°C	150°C	175°C	200°C	250°C	300°C	350°C
$\text{HgS}(\beta) - \text{H}_2\text{O}$	$\pm \text{Hg}$ $\pm \text{S}$	-1,87 +2,90	-3,07 +2,03	-0,15 +4,06	-3,20 +1,52	-3,33 -0,72	-3,14 +0,94	-3,36 +0,36	-0,89 +1,16	-2,88 +1,01	-3,52 +1,52	-1,88 +0,58
$\text{HgS}(\beta) - \text{Na}_2\text{S}(\text{aq})$	$\pm \text{Hg}$ $\pm \text{S}$	-2,35 +1,16	-2,09 -1,52	-2,78 +4,92	-2,89 +0,14	-3,32 +0,72	-3,40 +1,52	-2,77 -2,54	-3,20 -0,42	-3,14 -0,43	-2,91 -0,97	-2,26 -0,07
$\text{HgS}(\beta) - \text{AsCl}_3(\text{aq})$	$\pm \text{Hg}$ $\pm \text{S}$	-3,91 -3,26	-2,10 +1,88	-1,73 +5,00	-3,27 +5,00	-1,91 +5,87	-1,82 +5,43	-1,47 +2,46	-2,08 +7,32	-2,44 +7,97	-0,82 +3,84	-
$\text{HgS}(\beta) - \text{SbCl}_3(\text{aq})$	$\pm \text{Hg}$ $\pm \text{S}$	-0,07 +0,22	-1,21 +1,09	-0,38 -0,22	-0,60 +0,72	-2,27 +1,09	-2,95 +0,29	-0,53 +1,38	-0,53 +0,87	-1,87 0,00	-0,14 -0,71	-
$\text{HgS}(\beta) - \text{TlCl}(\text{aq})$	$\pm \text{Hg}$ $\pm \text{S}$	-2,77 -0,65	-2,30 -0,22	-2,89 +2,39	-1,54 -1,23	-1,35 -1,88	-0,15 +0,29	-1,97 -0,65	-3,62 +0,72	-2,97 +0,58	-2,15 -0,94	-2,95 +1,23

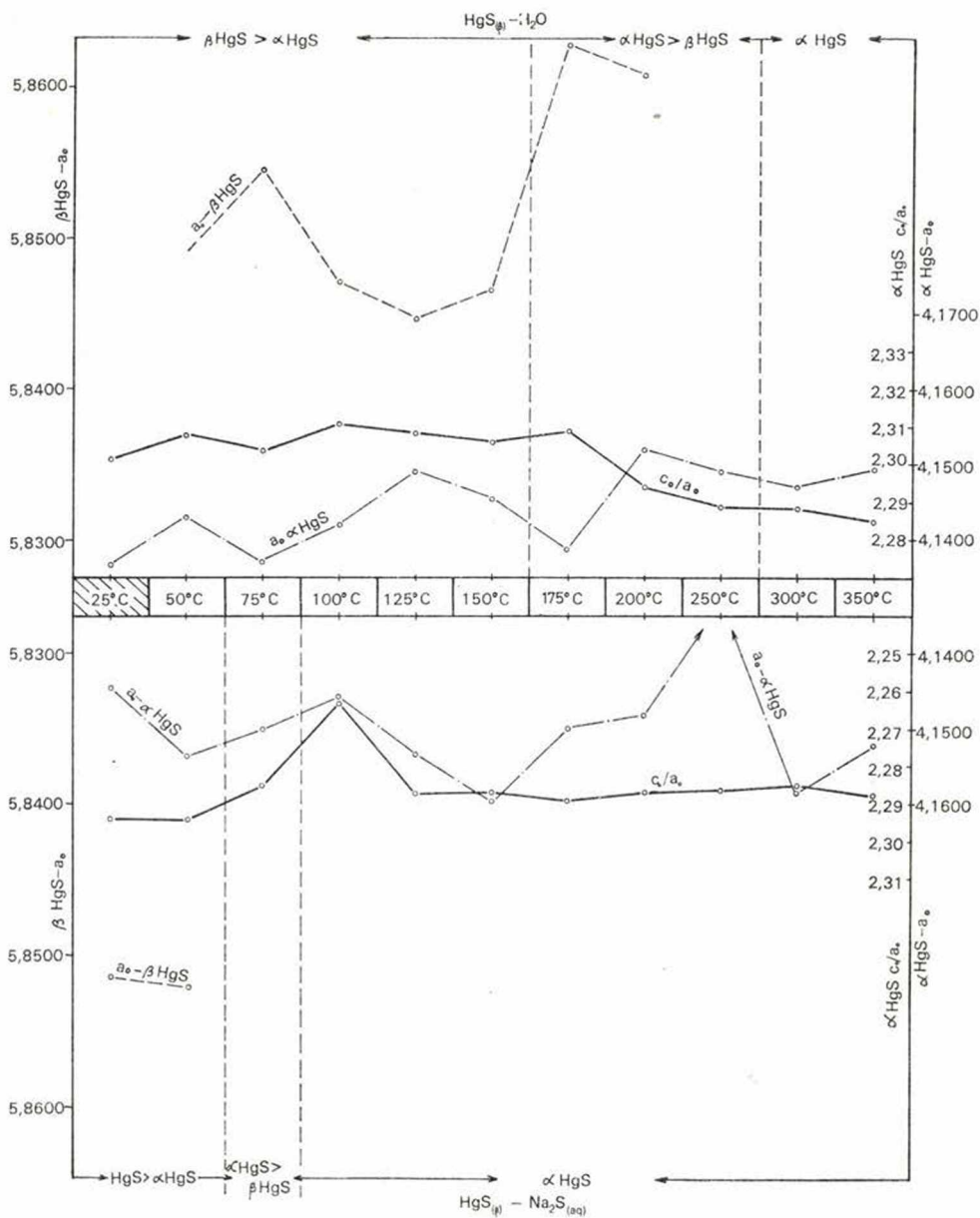


Fig. 6. Structural parameter variations of crystal phases of $\text{HgS}_{(s)}-\text{H}_2\text{O}$ and $\text{HgS}_{(s)}-\text{Na}_2\text{S}_{(aq)}$

4. Experiments with the formation of (Hg, R) S from $HgCl_{2(aq)} + R\text{-chloride} + H_2S$ and $HgS_{(s)} + R\text{-chloride system}$ (R = As, Sb, Tl)

4.1. $HgCl_{2(aq)} - AsCl_3 - H_2S_{(s)}$ ($25^\circ, 50^\circ, 75^\circ, 100^\circ C$)

a) Hg : As = 100 : 1

b) Hg : As = 1000 : 1

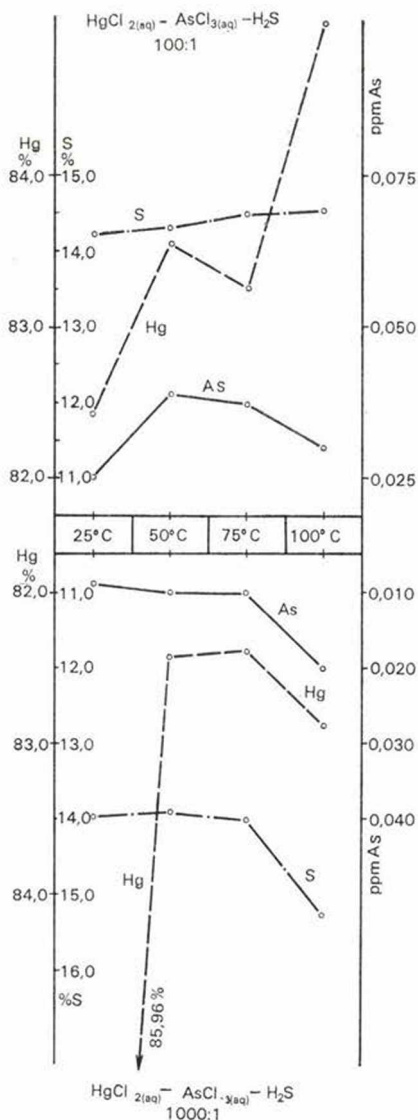


Fig. 7. Analysis data of $HgCl_{2(aq)} - AsCl_{3(aq)} - H_2S$ system

The crystalline product both systems (100:1, 1000:1) is powder-like black. The crystalline phase is βHgS , which contained about 2–3 per cent $\gamma\text{Hg}_3\text{S}_2\text{Cl}_2$ impurities. It seems that with rising temperature the Hg , As and S exhibit little of any variation. Data of analyses are summarised in Fig. 7. The largest differences were recorded in Hg -content in the experiments at 25°C and 100°C. The closest correlation of Hg - As - S have been observed in the 1000 : 1 = $Hg:As$ system (Fig. 7).

The average values of the analysis:

100 : 1	83.56% Hg ;	14.38% S ,	0.032% As
1000 : 1	83.38% Hg ;	14.30% S ;	0.012% As
(pH of the solution: 0.64–0.61)			

The non-stoichiometric distribution of Hg – S in crystalline phase is almost unaffected by the As content (Table IV., and VI).

100 : 1	$Hg = -3.11\%$	$S = +4.20\%$	$As = 0.03\%$
1000 : 1	$Hg = -3.27\%$	$S = +3.64\%$	$As = 0.01\%$

The largest Hg deficiency is in the 100:1 system at 100°C and in the 1000 : 1 system at 25°C, in βHgS phases. The βHgS cell-parameters are the smallest in this system, (average values)

100 : 1	= 327,5 ppm As ,	$a_0 = 5.8396 \text{ \AA}$
1000 : 1	= 122,5 ppm As ,	$a_0 = 5.8415 \text{ \AA}$

The difference between $Hg^\circ = 1.51 \text{ \AA}$ and $As^\circ = 1.48 \text{ \AA}$ is small, hence substitution does not necessarily cause change in the cell parameters. However, the larger difference between $Hg^+ = 1.10 \text{ \AA}$ and $As^{3+} = 0.58 \text{ \AA}$ caused cell contraction at 100–300 ppm As content.

The 100 : 1 system contains 327.5 ppm As , this explains the small average a_0 values in βHgS . Fig. 8. shows that a_0 values are smaller than literature data and among the experimental data the smallest values have been obtained by no means in this system.

4.2 $HgS_{(s)} + AsCl_{3(aq)} - 100 : 1$

The crystallised products of the $HgS_{(s)} - AsCl_{3(aq)}$ system can be grouped in distinct temperature intervals. The mean values of analysis are arranged according to the increasing temperature (Fig. 9).

- 25–150°C = βHgS
- 175°C = $\beta\text{HgS} > \alpha\text{HgS}$
- 200–250°C = $\alpha\text{HgS} > \beta\text{HgS}$
- 300°C = αHgS

- 25°–150°C = 84.08% Hg , 14.08% S , 20 ppm As
(pH = 1.56–1.67)
- 175°C = 84.93% Hg , 14.14% S , 15 ppm As
(pH = 1.36)

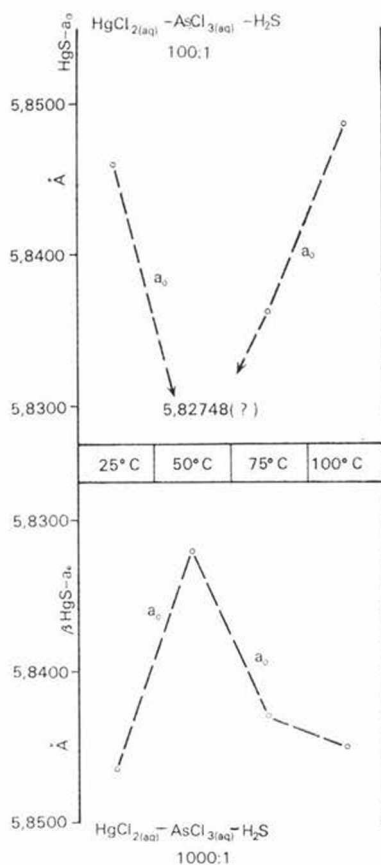


Fig. 8. Cell-parameters in $\text{HgCl}_2(aq) - \text{AsCl}_3(aq) - \text{H}_2\text{S}$ system

- c) $200 - 250^\circ\text{C} = 84.26\% \text{ Hg}, 14.86\% \text{ S}, 12.5 \text{ ppm As}$
 (pH = 1.36)
- d) $300^\circ\text{C} = 85.49\% \text{ Hg}, 14.33\% \text{ S}, 10.0 \text{ ppm As}$
 (pH = 1.45)

With increasing temperature the crystalline phases which contain 97–98% HgS show relative increase of HgS content and decreasing of As . The Hg -deficiency is decreasing the S -surplus is increasing contemporaneously, with the following average values in $\alpha\text{HgS} - \beta\text{HgS}$ phases:

- a) $25^\circ - 150^\circ\text{C} = -2.46\% \text{ Hg}, +4.61\% \text{ S} \quad 20 \text{ ppm As},$
 b) $175^\circ\text{C} = -1.47\% \text{ Hg}, +2.96\% \text{ S} \quad 15 \text{ ppm As},$
 c) $200^\circ - 250^\circ\text{C} = -2.26\% \text{ Hg}, +7.64\% \text{ S} \quad 12.5 \text{ ppm As},$
 d) $300^\circ\text{C} = -0.82\% \text{ Hg}, +3.84\% \text{ S} \quad 10.0 \text{ ppm As},$
 (from Table V).

Table VI.
The non-stoichiometric composition of the HgS

System	βHgS		αHgS		$\beta\text{HgS} > \alpha\text{HgS}$		$\alpha\text{HgS} > \beta\text{HgS}$	
	$\pm\text{Hg}$	$\pm\text{S}$	$\pm\text{Hg}$	$\pm\text{S}$	$\pm\text{Hg}$	$\pm\text{S}$	$\pm\text{Hg}$	$\pm\text{S}$
$\text{Hg}(\text{NO}_3)_{(aq)} - \text{H}_2\text{S}$	-	-	+3,97	-23,05(1)	-	-	-	-
$\text{HgCl}_{2(aq)} - \text{H}_2\text{S}$	-1,33	+1,38	-	-	-1,65	-3,91	-	-
$\text{HgCl}_{2(aq)} - \text{AsCl}_{3(aq)} - \text{H}_2\text{S}$	-3,19	+3,80	-	-	-	-	-	-
$\text{HgCl}_{2(aq)} - \text{SbCl}_{3(aq)} - \text{H}_2\text{S}$	-5,22	-4,34	-	-	-	+8,50	-	-
$\text{HgCl}_{2(aq)}\text{TlCl}_{(aq)} - \text{H}_2\text{S}$	-3,71	+2,79	-	-	-3,51	+2,68	-	-
$\text{HgS}(\beta) - \text{H}_2\text{O}$	-	-	-2,70	+1,05	-2,46	+2,03	-2,38	+0,84
$\text{HgS}(\beta) - \text{Na}_2\text{S}$	-	-	-2,98	+1,09	-2,22	+0,18	-2,51	+2,14
$\text{HgS}(\beta) - \text{AsCl}_3 - \text{H}_2\text{O}$	-2,29	+4,24	-1,63	+5,91	-1,47	+2,46	-2,08	+7,32
$\text{HgS}(\beta) - \text{SbCl}_3 - \text{H}_2\text{O}$	-0,68	+0,60	-1,01	-0,71	-2,61	+0,69	-0,53	+1,13
$\text{HgS}(\beta) - \text{TlCl} - \text{H}_2\text{O}$	-2,17	+0,40	-2,54	+1,09	-1,91	+0,36	-2,97	+0,58

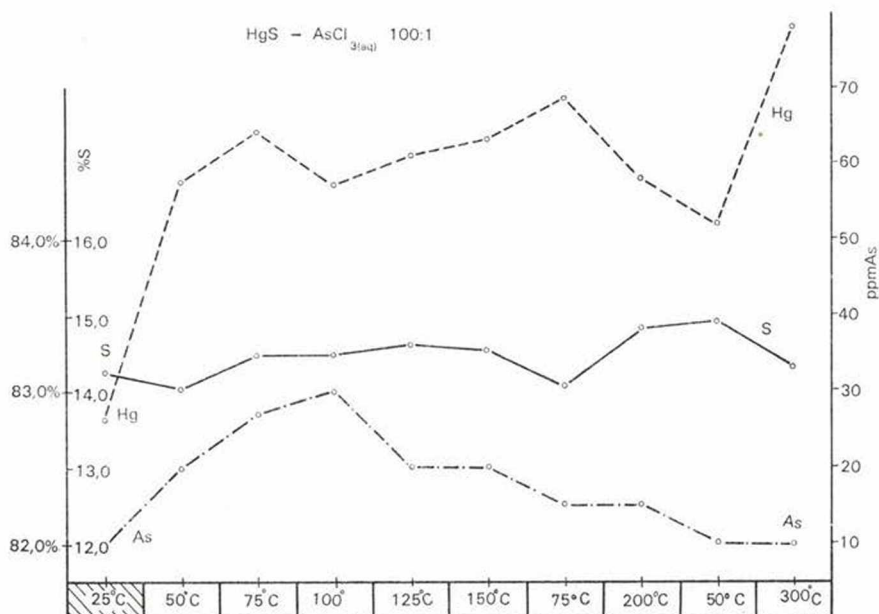


Fig. 9. Analysis of $\text{HgS}_{(s)} - \text{AsCl}_{3(aq)}$ as a function of T°

The crystalline product of reactions at $25^\circ - 150^\circ\text{C}$ is dominantly $\beta\text{Hg}_2\text{S}$, with 1–2 per cent of $\gamma\text{Hg}_3\text{S}_2\text{Cl}_2$ impurities. $\beta\text{Hg}_2\text{S} > \alpha\text{Hg}_2\text{S}$ has been formed at 175°C , $\alpha\text{Hg}_2\text{S} > \beta\text{Hg}_2\text{S}$ between 200°C and 250°C , pure $\alpha\text{Hg}_2\text{S}$ at 300°C . From the pure phases, $\beta\text{Hg}_2\text{S}$ is an average more deficient in $\text{Hg} - \text{S}$ than $\alpha\text{Hg}_2\text{S}$ (Table VI).

The cell-dimensions of $\beta\text{Hg}_2\text{S}$ are probably effected by the As content. The a_0 value of $\beta\text{Hg}_2\text{S}$ formed from solutions is smaller than those published in literature. After recrystallisation of the $\text{HgS}_{(s)} - \text{AsCl}_{3(aq)}$ system fall closer to these data. The values are increasing on higher temperatures:

$$\begin{aligned} 100 : 1 (25^\circ - 100^\circ\text{C}) &= a_0 = 5.8396 \text{ \AA} \\ 1000 : 1 (25^\circ - 100^\circ\text{C}) &= a_0 = 5.8415 \text{ \AA} \\ (175^\circ\text{C}) &= a_0 = 5.8545 \text{ \AA} \end{aligned}$$

The cell of $\alpha\text{Hg}_2\text{S}$ formed along with $\beta\text{Hg}_2\text{S}$ is more elongated than the c_0/a_0 of that one formed as mono-phase.

$$\begin{aligned} \beta\text{Hg}_2\text{S} > \alpha\text{Hg}_2\text{S} &= c_0/a_0 = 2.2918 \text{ \AA} \\ \alpha\text{Hg}_2\text{S} > \beta\text{Hg}_2\text{S} &= c_0/a_0 = 2.2909 \text{ \AA} \\ \alpha\text{Hg}_2\text{S} &= 2.2885 \text{ \AA} \end{aligned}$$

Results are summarized in Fig. 10.

4.3. $\text{HgCl}_{2(aq)} - \text{SbCl}_{3(aq)} - \text{H}_2\text{S} (25^\circ - 50^\circ - 75^\circ - 100^\circ\text{C})$

- $\text{Hg} : \text{Sb} = 100 : 1$
- $\text{Hg} : \text{Sb} = 1000 : 1$

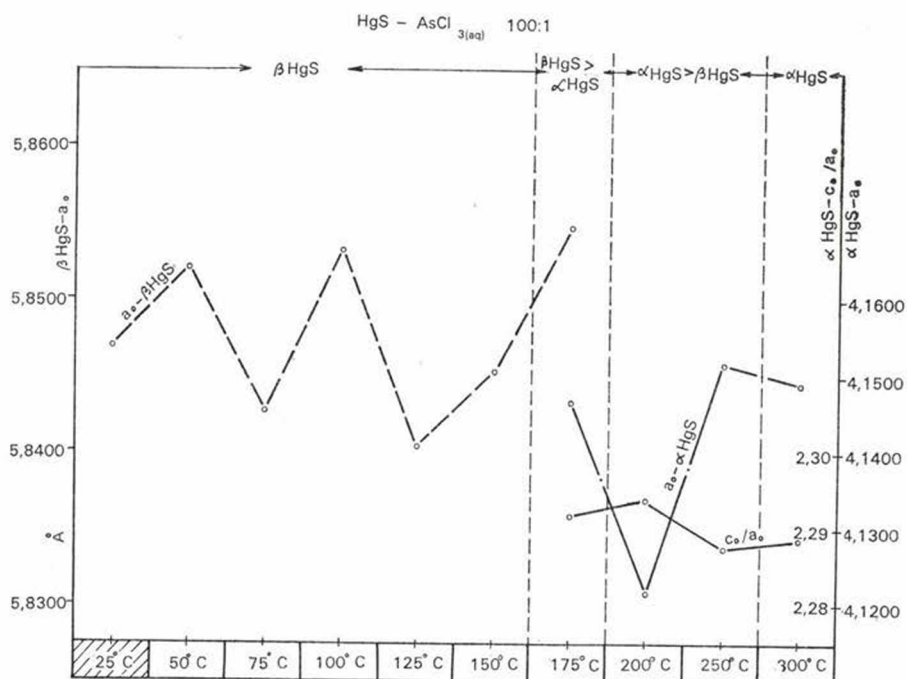


Fig. 10. Cell-parameters of crystalline-phases of $\text{HgS}_{(s)} - \text{AsCl}_{3(aq)}$ system

The antimony is the most abundant element associated with mercury mineralizations. Thus it seems reasonable to study the relationships of *Hg*-sulphides and antimony. The differences of atomic and ionic radii of the two elements:

$$\Delta = 0.15 \text{ \AA} \text{ (atomic radii)}$$

$$\Delta = 0.34 \text{ \AA} \text{ (ionic radii)*}$$

The metallic bonds of the two element might not cause considerable change in the structural framework while with ionic linkage structural distortions possibly arise.

Black, isometric, nearly square- or diamond shaped crystallites have been formed in the systems 100 : 1 and 1000 : 1 = *Hg* : *Sb*

100 : 1

25°C	black	βHgS	pH = 0.2
50°C	black	βHgS	pH = 0.2
75°C	black	βHgS	pH = 0.2
100°C	black	$\beta > \alpha\text{HgS}$	pH = 0.2

* = 0,22 Å at Whittaker - Muntus (1970)

1000 : 1

25°C	black	βHgS	pH = 0.2
50°C	black	βHgS	pH = 0.2
75°C	black	$\beta > \alpha\text{HgS}$	pH = 0.2
100°C	black	$\beta > \alpha\text{HgS}$	pH = 0.2

The monophase character of βHgS formed at 25°–50°C is typical to the $\text{HgCl}_{2(aq)}-\text{SbCl}_{3(aq)}-\text{H}_2\text{S}$ system (Similar to the $\text{HgCl}_2-\text{H}_2\text{S}$ system). From 75°C αHgS has also appeared, unlike with *As*. The amount of $\gamma\text{Hg}_3\text{S}_2\text{Cl}_2$ phase was orders smaller than in the $\text{HgCl}_{2(aq)}-\text{AsCl}_{3(aq)}-\text{H}_2\text{S}$ system. The analysis of crystalline phases are shown in Fig. 11. This indicates that there is close relationship between *Sb*–*S* in both system and among *Hg*–*Sb*–*S* in the 1000 : 1 = *Hg* : *Sb* system.

The *Hg*-deficiency of the crystalline phase is larger in the 100 : 1 system than in the 1000 : 1 system. Significant variation in *S* content has been observed (Fig. 11., Table IV). The average non-stoichiometric compositions.

100 : 1 = 82.62% <i>Hg</i> ;	14.71% <i>S</i> ;	0.77% <i>Sb</i>
1000 : 1 = 84.67% <i>Hg</i> ;	13.93% <i>S</i> ;	0.05% <i>Sb</i>

with differences of

100 : 1 = –4.15% <i>Hg</i> ;	+6.66% <i>S</i>
1000 : 1 = –1.47% <i>Hg</i> ;	+1.06% <i>S</i>

The greatest *Hg*-deficiency has been resulted in 100 : 1 system at 25°C and in 1000 : 1 system at 100°C. The *S* content in the 100 : 1 system has varied in the range of –0.07, +10.94 (Table IV., and VI).

The βHgS formed at 25°–100°C show cell dimensions nearly similar to literature data (being smaller, differs only in the third decimal):

100 : 1 = $\beta\text{HgS} = a_0 = 5.8472 \text{ \AA} = 7700 \text{ ppm } Sb$
1000 : 1 = $\beta\text{HgS} = a_0 = 5.8483 \text{ \AA} = 500 \text{ ppm } Sb$

The deformational effect of antimony can not be proved here. The distributions of cell parameters of βHgS follow similar trends both in system (100 : 1 and 1000 : 1), and show minimum at 100°C. (Fig. 12.)

4.4 $\text{HgS}_{(s)}-\text{SbCl}_{3(aq)}-100 : 1$

Mono-phase βHgS has formed at 25°–100°C, αHgS between 250°–300°C, and mixed phases in 100°C–250°C temperature range.

- 25–100°C = βHgS^*
- 125–150°C = $\beta\text{HgS} > \alpha\text{HgS}$
- 175–200°C = $\alpha\text{HgS} > \beta\text{HgS}$
- 250–300°C = αHgS

* Formation of αHgS in form of crystal nuclei has probably started at 50 °C, but its presence is still uncertain at 75 °C.

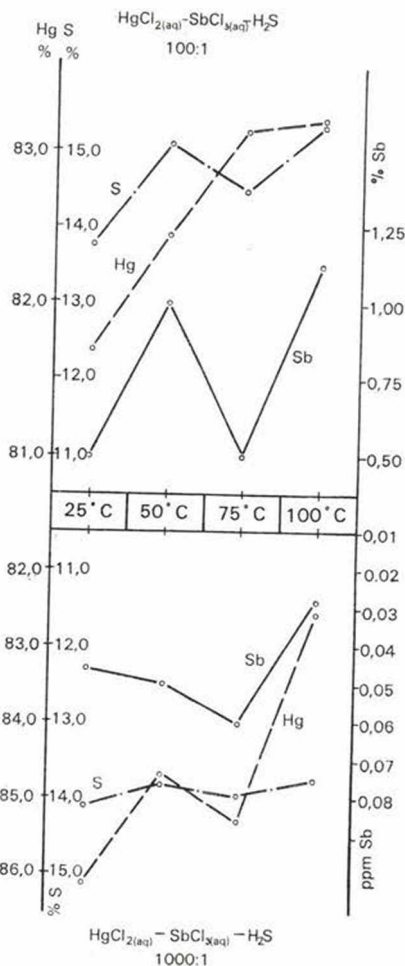


Fig. 11. Analysis data of $\text{HgCl}_2(aq) - \text{SbCl}_3(aq) - \text{H}_2\text{S}$ systems

1–2% $\text{Hg}_3\text{S}_2\text{Cl}_2$ is permanently present. From 75°C Sb_2S_3 was observed.

The $\text{Hg} : \text{Sb}$ ratio in the composition of crystallized material showed inverse relationships, antimony crystallises dominantly as separate phase (Sb_2S_3), and its incorporation to the HgS structure is restricted.

The average of analysis results based in the distribution of β - and α HgS phases:

- a) 25°–100°C = 85.74% Hg , 13.86% S , 2800 ppm Sb
 b) 125°–150°C = 83.95% Hg , 13.89% S , 300 ppm Sb
 c) 175°–200°C = 85.74% Hg , 13.83% S , 30 ppm Sb
 d) 250°–300°C = 85.28% Hg , 13.85% S , 10 ppm Sb (Fig. 13.)

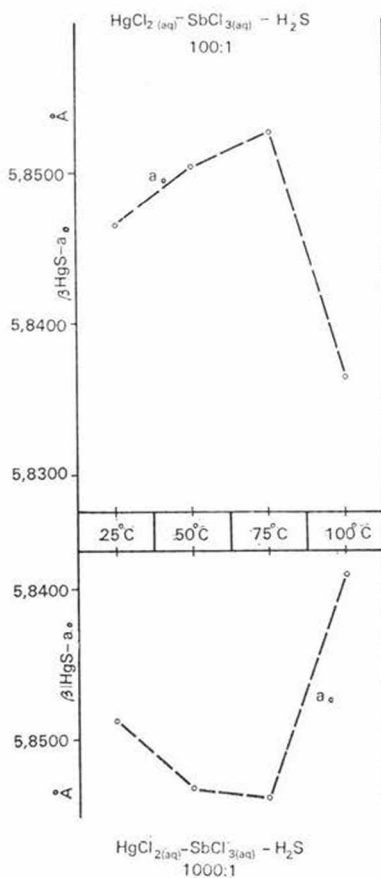


Fig. 12. HgS cell-parameters
in the $\text{HgCl}_{2(aq)}-\text{SbCl}_{3(aq)}-\text{H}_2\text{S}$ systems

The $\text{HgS}_{(s)}-\text{SbCl}_3$ system shows the smallest Hg - and S deficiency. The $Hg:S$ ratio exhibits close relationship with stoichiometric values (based on data from Table V and VII).

- a) $25^\circ-100^\circ = 0,76 Hg, +0,60 S$
- b) $125^\circ-150^\circ = -2,61 Hg, +0,64 S$
- c) $175^\circ-200^\circ = -0,53 Hg, +1,13 S$
- d) $200^\circ-300^\circ = -1,00 Hg, -0,35 S$

Above 200°C the $\text{HgS}_{(s)}+\text{SbCl}_{3(aq)}$ system is characterised by α HgS phases having a special crystal-morphology. The average size of crystal grains is $0,2-0,5$ mm with maximum of $1,0$ mm. The antimony catalyses the inversion of βHgS to cinnabar significantly. At 300°C the rate of Sb impurity is only 10 ppm.

The a_0 parameter: of the metacinnabar (βHgS) phases form $\text{HgS}_{(s)} - \text{SbCl}_{3(aq)}$ system averaging the following values:

- a) $25^\circ\text{C} - 100^\circ\text{C} = a_0 = 5.8457 \text{ \AA}$, 2800 ppm Sb
 b) $125^\circ\text{C} - 150^\circ\text{C} = a_0 = 5.8542 \text{ \AA}$, 200 ppm Sb
 c) $175^\circ\text{C} - 200^\circ\text{C} = a_0 = 5.8563 \text{ \AA}$, 30 ppm Sb

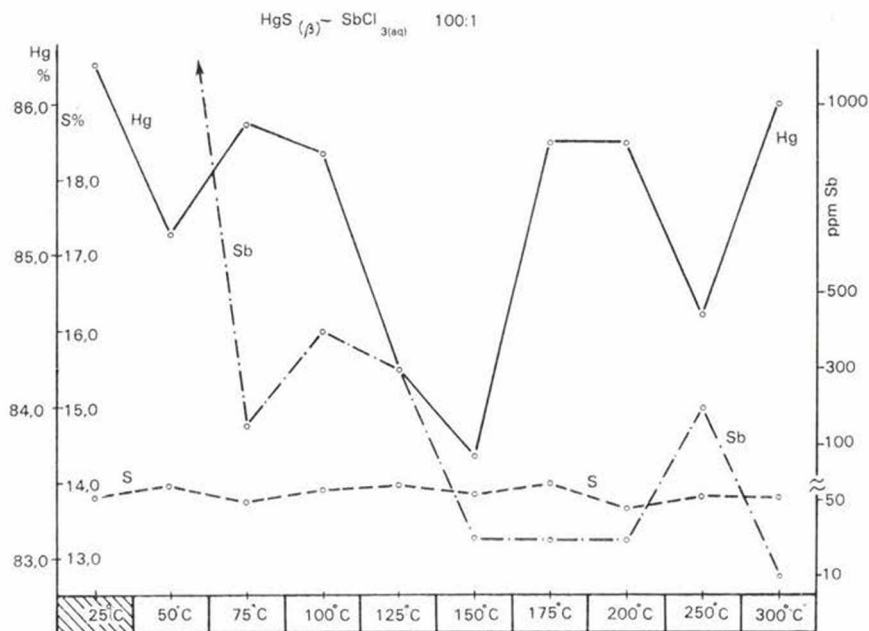


Fig. 13. Analysis data of crystalline phases of $\text{HgS} - \text{SbCl}_{3(aq)}$ as a function of T°

It seems that αHgS contains less *As* and *Sb* than βHgS with sphalerite-structure. The distributions of structural parameters of βHgS and αHgS are summarized in Fig. 14.

4.5. $\text{HgCl}_{2(aq)} - \text{TlCl}_{(aq)} - \text{H}_2\text{S} (25^\circ - 50^\circ - 75^\circ - 100^\circ\text{C})$

- a) $\text{Hg} : \text{Tl} = 100 : 1$
 b) $\text{Hg} : \text{Tl} = 1000 : 1$

Both mercury and thallium tends to concentrate in epithermal deposits but only few data had been published about their genetical, geo-chemical relationship. For crystal-chemical reasons thallium has favourable characteristics to be in close association with mercury. There is only minute difference between the atomic radii:

$$\text{Hg}^\circ = 1.51 \text{ \AA}, \quad \text{Tl}^\circ = 1.60 \text{ \AA} \quad \Delta = 0.09$$

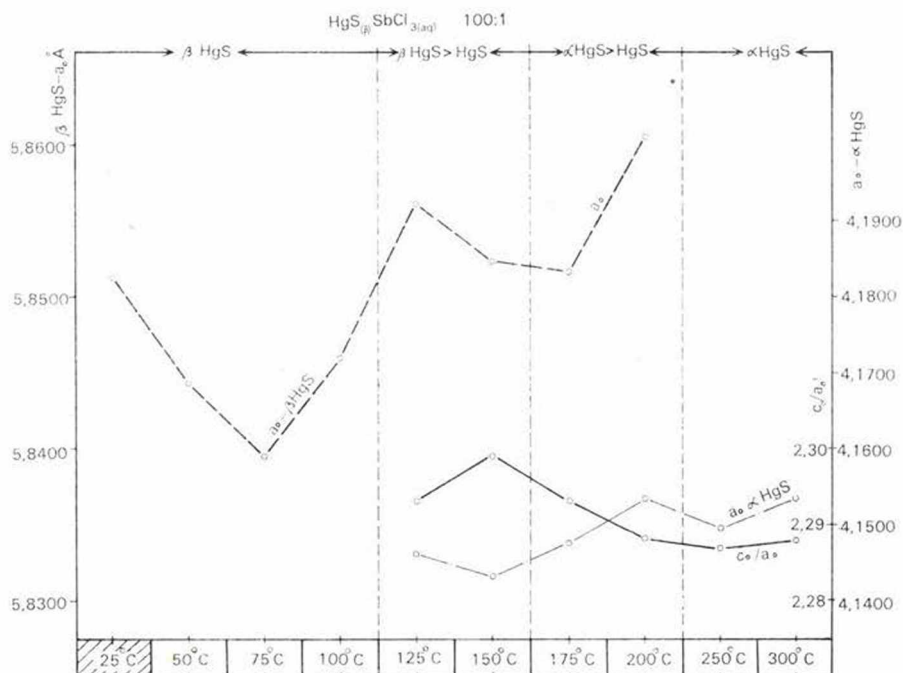


Fig. 14. Structural parameters of phases in $\text{HgS}_{(s)} - \text{SbCl}_{3(aq)}$ systems

The differences of ionic radii still permit isomorphous substitution:

$$\text{Hg}^{2+} = 1.10 \text{ \AA}, \quad \text{Tl}^+ = 1.47 \text{ \AA} \quad \Delta = 0.37 \text{ \AA}^*$$

The products of 100 : 1 and 1000 : 1 systems are black isometric, nearly square-shaped grains and lamellae. At larger Tl-content (100:1) only βHgS has been formed. In 1000 : 1 = Hg : Tl system at 75°–100°C αHgS has also appeared, similarly to the $\text{HgCl}_2 - \text{H}_2\text{S}$ system:

100 : 1

25°C =	black	βHgS	pH = 1.30
50°C =	black	βHgS	pH = 1.31
75°C =	black	βHgS	pH = 1.35
100°C =	black	βHgS	pH = 1.25

1000 : 1

25°C =	black	βHgS	pH = 1.30
50°C =	black	βHgS	pH = 1.30
75°C =	black	$\beta > \alpha\text{HgS}$	pH = 1.29
100°C =	black	$\beta > \alpha\text{HgS}$	pH = 1.20

$\gamma\text{Hg}_3\text{S}_2\text{Cl}_2$ as associated phase has appeared only at 100°C in the 1000 : 1 system. In other cases only HgS has been crystallised. The chlorine content

* $\Delta = 0.48 \text{ \AA}$ at Whittaker - Muntus (1970)

of the crystalline phases is averaging at 0.11%, in few cases 0.05% or less has been analysed. From all Hg-solution-vapor systems studied the HgS phases of the $\text{HgCl}_{2(aq)}-\text{TlCl}_{(aq)}$ system showed the highest deficiency in Hg and S, though Hg:S ratio is more permanent in this system than in others.

Maximum Hg-content has been recorded in sulphide phases at 75°C. in both systems (100:1 and 1000:1).

The Hg:S ratio is the closest to stoichiometric ratios in this case. Analyses are summarised in Fig. 15.

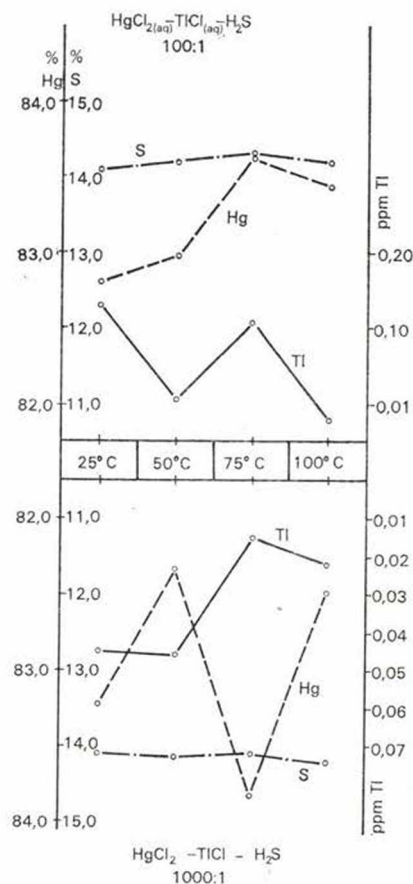


Fig. 15. Analysis data of the phases from $\text{HgCl}_{2(aq)}-\text{TlCl}_{(aq)}-\text{H}_2\text{S}$ systems

The crystalline phases show Hg deficiency and S surplus with permanent difference. (Table IV).

The average of analysis data:

$$\begin{aligned} 100 : 1 &= 83.24\% \text{ Hg}, 14.25\% \text{ S } 800 \text{ ppm Tl} \\ 1000 : 1 &= 25^\circ - 50^\circ = 82.80\% \text{ Hg}, 14.12\% \text{ S}, 460 \text{ ppm Tl} \\ &= 75^\circ - 1000^\circ = 83.17\% \text{ Hg}, 14.51\% \text{ S}, 180 \text{ ppm Tl} \end{aligned}$$

wich is equal to:

$$\begin{aligned} 100 : 1 &= - 3.47\% \text{ Hg}, + 3.34\% \text{ S} \\ 1000 : 1 &= 25^\circ - 50^\circ \text{C} = - 3.99\% \text{ Hg} + 2.32\% \text{ S} \\ &75 - 1000^\circ \text{C} = - 3.02\% \text{ Hg} + 2.68\% \text{ S} \end{aligned}$$

deficiency and surplus.

The cell-parameter of βHgS phase is averagely larger than the literature data in the second decimal. As smallest a_0 values have been obtained with As , the largest ones with Tl , it is suggested that cell-deformation effect of ionic radii $Tl > Sb > As$, have been responsible for theses differences in case of ionic bonds:

$$\begin{aligned} 100 : 1 &= \beta\text{HgS} = a_0 = 5.8627 \text{ \AA} - 800 \text{ ppm Tl} \\ 1000 : 1 &= \beta\text{HgS} = a_0 = 5.8506 \text{ \AA} - 460 \text{ ppm Tl} \end{aligned}$$

The variation of a_0 values is shown in Fig. 16.

4.6 $\text{HgS}_{(aq)} - \text{TlCl}_{(aq)} - 100 : 1$

During the experiments mixed $\beta > \alpha$ and $\alpha > \beta$ HgS phases have been formed in wide temperature interval ($150^\circ - 250^\circ\text{C}$):

- a) $25^\circ - 125^\circ\text{C} = \beta\text{HgS}$ pH = 4.56 - 2.56 (black)
- b) $150^\circ - 200^\circ\text{C} = \beta\text{HgS} > \alpha \text{HgS}$ pH = 2.65 - 2.52 (black)
- c) $250^\circ\text{C} = \alpha\text{HgS} > \beta \text{HgS}$ pH = 2.50 (brownish-red)
- d) $300^\circ - 350^\circ\text{C} = \beta\text{HgS}$ pH = 2.57 - 2.60 (purple).

With rising temperature the acidity of the solution is increasing, βHgS is converting to αHgS . The Hg -content of sulfide phases shows maximum $100^\circ - 150^\circ\text{C}$ and minimum at 200°C . (Fig. 17).

The Tl content is gradually decreasing with temperature, while the amount of S remains practically unchanged. (Table V and VI).

The average values of analysis data shown in Fig. 17.

- a) $25^\circ - 125^\circ\text{C} = 84.33\% \text{ Hg}, 13.76\% \text{ S } 400 \text{ ppm Tl}$
- b) $150^\circ - 200^\circ\text{C} = 84.55\% \text{ Hg}, 13.81\% \text{ S } 200 \text{ ppm Tl}$
- c) $250^\circ\text{C} = 83.64\% \text{ Hg}, 13.88\% \text{ S } 70 \text{ ppm Tl}$
- d) $300^\circ - 350^\circ\text{C} = 84.01\% \text{ Hg}, 13.95\% \text{ S } 100 \text{ ppm Tl}$

wich are equal to:

- a) $25^\circ - 125^\circ\text{C} = - 2.16\% \text{ Hg} - 0.53\% \text{ S}$
- b) $150^\circ - 200^\circ\text{C} = - 1.91\% \text{ Hg} + 0.04\% \text{ S } (*)$
- c) $200^\circ\text{C} = - 1.91\% \text{ Hg} + 0.04\% \text{ S } (*)$
- d) $300^\circ - 350^\circ\text{C} = - 2.55\% \text{ Hg} + 1.08\% \text{ S}$

* based on one analysis only

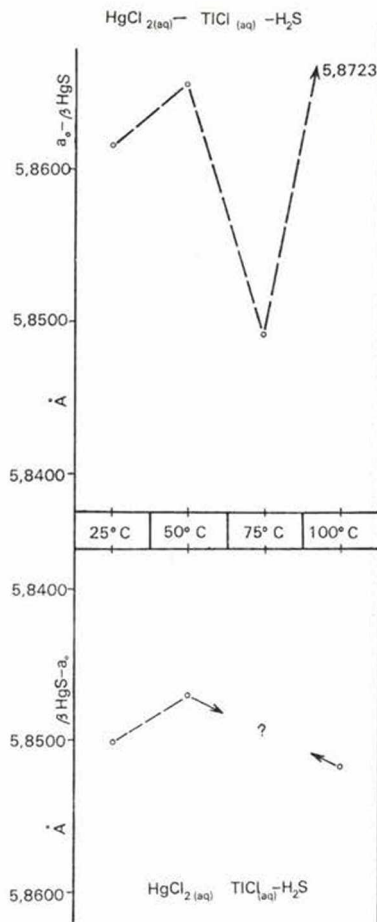


Fig. 16. Variation of cell-parameters in $\text{HgCl}_2(aq) - \text{TlCl}(aq) - \text{H}_2\text{S}$

These data indicated as temperature was increasing ($150^\circ - 200^\circ$), the difference in $\text{Hg} : \text{S}$ becoming smaller, then after αHgS became dominant, the difference was again larger (Table V.).

The cell-parameters of βHgS has been the largest among the systems studied:

- $25^\circ - 125^\circ\text{C} = a_0 = 5.8646 \text{ \AA} - 400 \text{ ppm Tl}$
- $150^\circ - 200^\circ\text{C} = a_0 = 5.8614 \text{ \AA} - 200 \text{ ppm Tl}$
- $250^\circ\text{C} = a_0 = 5.8613 \text{ \AA} - 70 \text{ ppm Tl}$

With rising temperature the a_0 values are decreasing along with the Tl content.

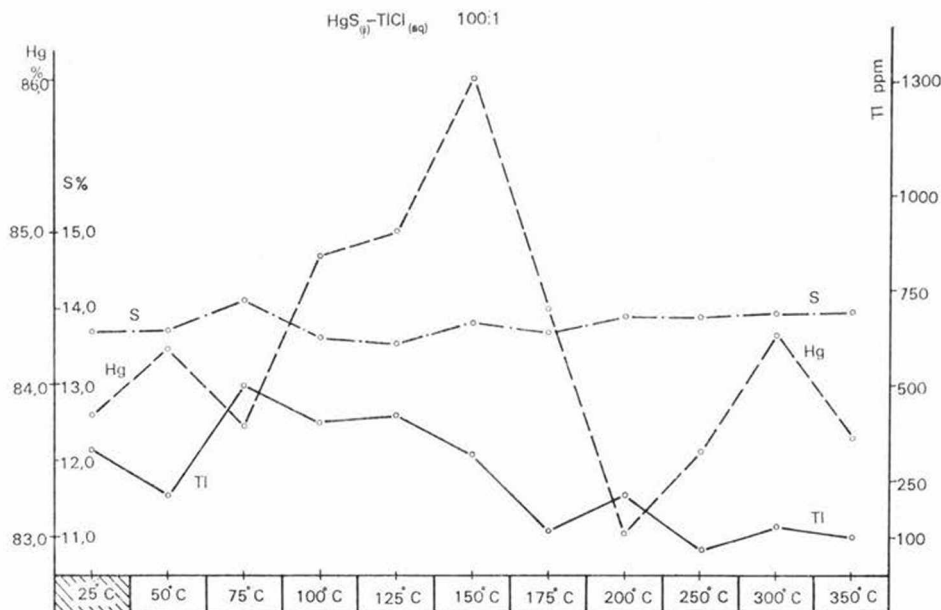


Fig. 17. Analysis data of crystalline phases of the $\text{HgS}_{(s)} - \text{TlCl}_{(aq)}$ system as a function of T°

The a_0 and c_0 parameters of αHgS are larger than literature data ($= 2.91 \text{ \AA}$), and indicate slight elongation in c_0 direction:

$150^\circ\text{C} - \text{HgS}$, $c_0/a_0 = 2.305$; $175^\circ\text{C} = 2.298$; $200^\circ\text{C} = 2.295 \text{ \AA}$
 $250^\circ\text{C} - \text{HgS}$, $c_0/a_0 = 2.292$; $300^\circ\text{C} = 2.287$; $350^\circ\text{C} = 2.286 \text{ \AA}$

The variations of βHgS and αHgS cell parameters are shown in Fig. 18.

5. Conclusions

The experiments have provided new explanations for the conditions of formation of βHgS and αHgS and the crystal-chemical mechanism of their conversion. The following problems had to be answered.

1. Why both modifications were usually formed in one paragenetical sequence, and which is the primarily precipitated mercury-sulfide, βHgS or αHgS .

2. Is the βHgS of shalerite-type structure the more metastable variety?

3. Is there any possibility for conversion of cinnabar to metacinnabar below the temperature of the inversion point (344°C).

4. Which of the crystal-chemical data are characteristic for βHgS and αHgS phases.

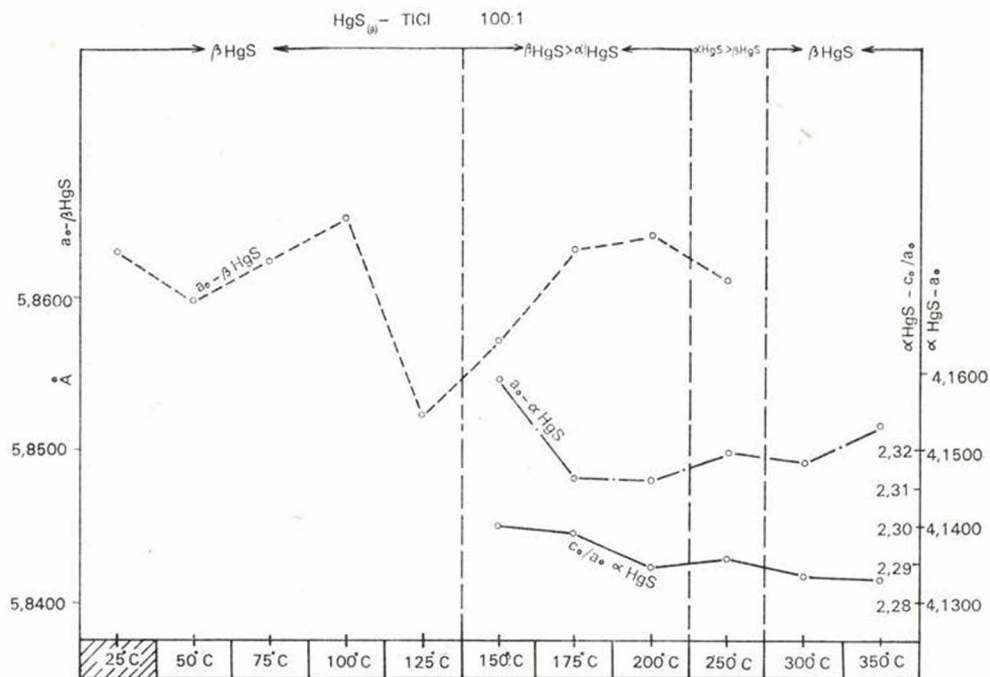


Fig. 18. Metacinnabar and cinnabar cell-parameters in the $\text{HgS}_{(s)} - \text{TlCl}_{(aq)}$ -system as a function of T°

5. Is there any role of the *As*, *Sb*, *Tl* impurities applied in the experiments on the formation of βHgS and αHgS . Do they have any effect on the cell-parameters?

6. What are the preconditions of alteration of βHgS to αHgS at room temperature. The aqueous media or the Na_2S solution in which βHgS has higher solubility is the more favourable solvent for this alteration?

These questions have been remained in most part unanswered in the previous literature of Hg-sulphide mineralization.

a) Between $25^\circ - 75^\circ\text{C}$. The mercury, mobilized in form of complexes by chloride the most abundant anion of hydrothermal solutions crystallises as βHgS of sphalerite-type structure. The coexistent crystallization of βHgS and αHgS in the temperature range of $75^\circ - 100^\circ\text{C}$ indicates that the formation of the more stable cinnabar-structure does not begin at room temperatures. In the $75^\circ - 100^\circ\text{C}$ experiments only βHgS had been produced in the first short intervals, i.e. 15–60 min. Only initial crystallites of αHgS has developed in the 8-hours experiments, as evidenced by the presence of the most intense $3.59 \text{ d}/\text{\AA}$ line and $1.735 \text{ d}/\text{\AA}$ doublet close to the $1.764 \text{ d}/\text{\AA}$ line of metacinnabar on the X-ray diffractograms.

From mercury (I)-nitrate solutions however αHgS , cinnabar has been formed at $25^\circ - 50^\circ\text{C}$, suggesting that the orbital character of the Hg/I- nitrate complex has governing effect on the development of structural type of mercury-sulfide.

In the experiments with $\text{HgNO}_{3(aq)} - \text{H}_2\text{S}$ at $75^\circ - 100^\circ\text{C}$ abrupt changes have been recorded in the proportion of mercury-sulfide polymorphs ($= \beta\text{HgS} > \alpha\text{HgS}$). The test had been repeated at 65°C and similar, $\beta\text{HgS} > \alpha\text{HgS}$ ratio has been obtained. In nitrate-containing solution vapor systems the inversion point can be positioned in $50 - 65^\circ\text{C}$ temperature range, in which mixed phases, $\beta\text{HgS} > \alpha\text{HgS}$ are crystallising, after αHgS was formed between $25^\circ - 50^\circ\text{C}$. In the case of nitrate-containing hydrothermal solutions the cinnabar and not the metacinnabar crystallises primarily below 50°C .

b) The As^{3+} ions in solution-vapor hydrothermal systems (at $25^\circ - 100^\circ\text{C}$) prevent formation of αHgS , while in cases of presence of Sb^{3+} and Tl^+ mono-phase βHgS has formed between $25^\circ - 50^\circ\text{C}$, and $\beta\text{HgS} > \alpha\text{HgS}$ polyphases at $75^\circ - 100^\circ\text{C}$, similarly to the $\text{HgCl}_2 - \text{H}_2\text{S}$ system.

c) The experiments showed that the first crystallites, formed from solution-vapor systems, have always, βHgS structure initially, then in presence of nitrate ions, these rapidly (5–6 hours) alter to αHgS , which is stable below 60°C . In case of excess chloride-content, metacinnabar is formed below 50°C , above this temperature coexisting αHgS is also present, $\beta\text{HgS} : \alpha\text{HgS}$ ratio is 4 : 1.

d) Hg-depleted sulfide-phases are formed from solution-gas system, which become structurally ordered in solid-liquid ($\text{HgS} + \text{metal-containing solutions}$) systems. The Hg-deficiency is larger in phases of metacinnabar structure, the Hg : S ratios show greater differences than in phases of cinnabar structure. In solid-phase – solution systems the Hg : S values are closer to the theoretical 1 : 1 ratio. This is most apparent for the cinnabar.

e) The recrystallisation of metacinnabar in solutions starts at room-temperature (30 days), through transitional mixed phases ($\alpha\text{HgS} > \beta\text{HgS}$) with cinnabar dominance at 175°C and to final mono-phase system at 300°C .

f) In the $\text{HgS}_{(s)} - \text{Na}_2\text{S}_{(s)}$ system at 100°C mono-phase αHgS is produced. Its formation begins at room temperature.

g) The metacinnabar to cinnabar alterations in Na_2S are stimulated by the presence of antimony (Sb^{3+}) ions. The alteration begins at 125°C .

h) In $\text{HgS}_{(s)} - \text{SbCl}_{3(aq)}$ systems large (few millimeters in size) crystals have formed.

i) At our experimental conditions alteration of cinnabar to metacinnabar has not been recorded. In close system this alteration takes place at 344°C . At present there are no observations for alteration of cinnabar to metacinnabar during termometamorphosis.

j) In natural environment for the primary formation of metacinnabar chloridic hydrothermal solutions have been proved to be the most favorable with As^{3+} content below 100°C , Tl^+ content below 25°C , Sb^{3+} content below 50°C . The metacinnabar to cinnabar alteration may take place by

post-ore hydrothermal effects depending on temperature and ion-concentration of the solution, and possibly follows one of these schematic processes:

I. $HgS + H_2O$

- a) $25^\circ - 150^\circ C = \beta HgS > \alpha HgS$
- b) $175^\circ - 250^\circ C = \alpha HgS > \beta HgS$
- c) $300^\circ C = \alpha HgS$

II. $HgS + Na_2S + H_2O$

- a) $25^\circ - 50^\circ C = \beta HgS > \alpha HgS$
- b) $75^\circ C = \alpha HgS > \beta HgS$
- c) $100^\circ - 350^\circ C = \alpha HgS$

III. $HgS + AsCl_3 + H_2O$

- a) $25^\circ - 150^\circ C = \beta HgS,$
- b) $175^\circ C = \beta HgS > \alpha HgS$
- c) $200^\circ - 250^\circ C = \alpha HgS > \beta HgS,$
- d) $300^\circ C = \alpha HgS$

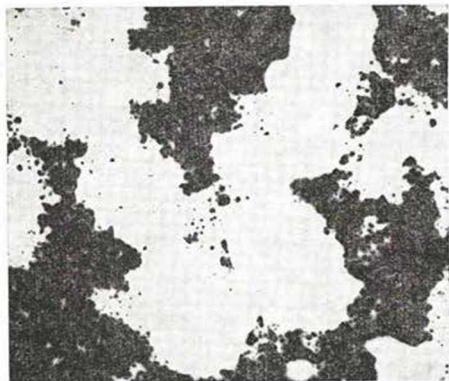
IV. $HgS + SbCl_3 + H_2O$

- a) $25^\circ - 100^\circ C = \beta HgS$
- b) $125^\circ - 150^\circ C = \beta HgS > \alpha HgS,$
- c) $175^\circ - 200^\circ C = \alpha HgS > \beta HgS$
- d) $250^\circ - 300^\circ C = \alpha HgS$

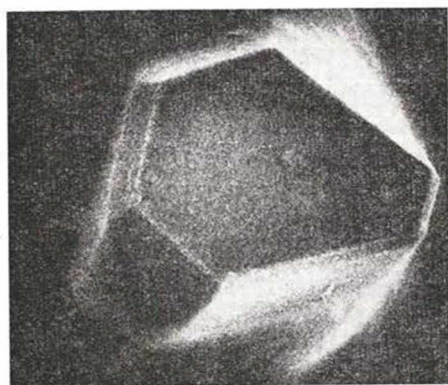
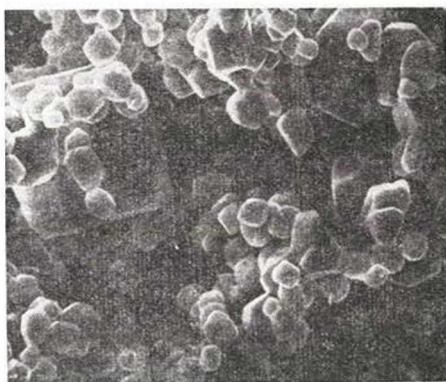
V. $HgS + TlCl + H_2O$

- a) $25^\circ - 125^\circ C = \beta HgS,$
- b) $150^\circ - 200^\circ C = \beta HgS > \alpha HgS,$
- c) $250^\circ C = \alpha HgS > \beta HgS,$
- d) $300^\circ - 350^\circ C = \alpha HgS.$

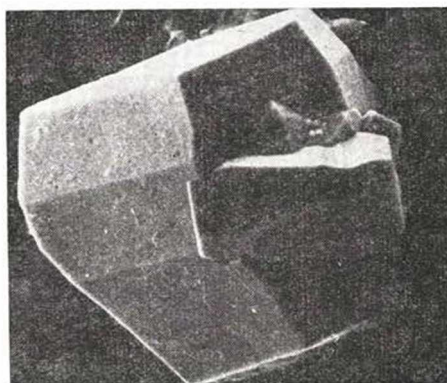
1



2



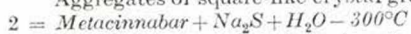
3



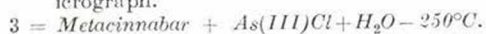
4



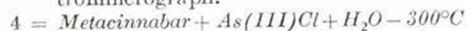
Aggregates of square-like crystal grains of Metacinnabar 120 \times .



Sub hexaedric, isometric grains of cinnabar with (0001) base planes; 10,000 \times , electronmicrograph.



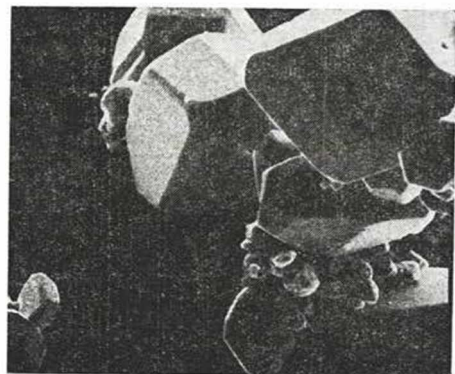
Idiomorphic cinnabar with (0001), (h0kl), (0hkl), and (1010) forms; 20 000 \times , electronmicrograph.



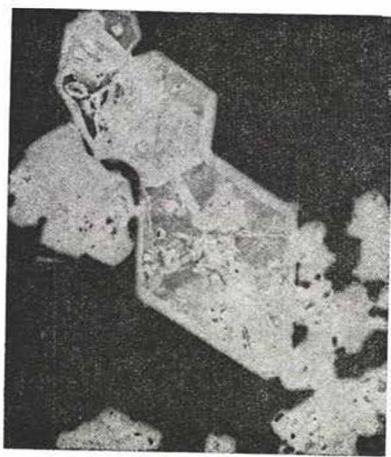
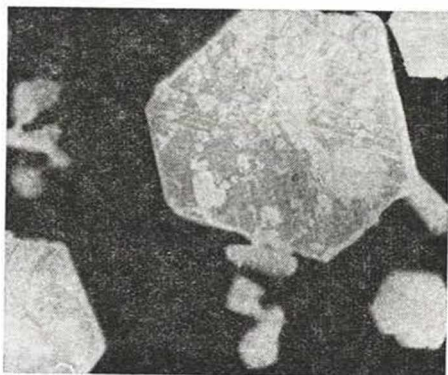
Idiomorphic cinnabar with different proto- and deutero romboheda and base-planes; Twin-intergrowth. 3000 \times ; electronmicrograph.

PLATE 2

5



6



7

5 = *Metacinnabar* + *Sb(III)Cl* + H_2O - $300^\circ C$.

Idiomorphic cinnabar (0001), (1010) planes. 3000x; electronmicrograph.

6 = *Metacinnabar* + *Sb(III)Cl* + H_2O - $250^\circ C$.

Powder-preparatum. cinnabar crystals (=0,5 mm) with crystal-growth characteristics; 80 x.

7 = *Metacinnabar* + *Sb(III)Cl* + H_2O - $300^\circ C$.

Powder-preparatum. cinnabar crystals (=0,5 mm) with crystal-growth characteristics; 80 x.

REFERENCES

- Barnes, H. L. et al. 1967: Ore solution chemistry II. etc. *Econ. Geol.* Vol. 62. p. 957—982.
- Cruceanu, E. et al. 1969: Crystal growth of HgS from Hg-rich solutions. *Journ. Cryst. Growth* (5); p. 206.
- Dickson, F. W., 1964: Solubility of cinnabar in Na₂S solutions at 50–250 °C and 1–1800 bars etc. *Econ. Geol.* Vol. 59. p. 625–635.
- Dickson, F. W. — Tunnel, G. 1958: Equilibria of red HgS and black HgS etc. *Am. Journ. Sci.* (256), p. 654.
- Dickson, F. W. 1959: The solubility relations of cinnabar and metacinnabar. *The Am. Min.* (44); p. 475.
- Dreyer, R. M. 1940: The geochemistry of quecksilber mineralization. *Econ. Geol.* Vol. 35; p. 17–48.
- Garner, R. W. et al. 1970: Growth of cinnabar from sodium sulfide. *Journ. Cryst. Growth* (7); p. 343–347.
- Krauskopf, K. B. 1951: Physical chemistry of quecksilber transportation in vein fluids. *Econ. Geol.* Vol. 46; p. 498–522.
- Ozerova, N. A. et al. 1969: Mercury mineralization at the Mendelyev Volcano. *Dokl. Ak. Sci. USSR. Earth Sci. Sect.* — 187; p. 652.
- Pajachovska, A. 1970: Hydrothermal crystallization of cinnabar *Journ. Cryst. Growth* (7); p. 93–96.
- Piotrovskii, G. L. 1961: One problem of genesis of cinnabar and metacinnabar. *Int. Geo. Review* (3); p. 652–657.
- Protodiakonova, Z. M. et al. 1971: O nekotorigh modifikaciah sulfida ruti etc. *Zap. Vsesoyuzn. Min. Obse. C.* 100; Vol. 6. p. 731–738.
- Saukov, A. A. 1973: *Geochemie.* VEB Verlag, Berlin.
- Schwarzenbach, S. — Widmer, M. 1963: Die Löslichkeit von Metasulfiden I. etc. *Helv. Chim. Acta.* Vol. 46; p. 2613–2628.
- Thompson, G. A. 1954: Transportation and deposition quicksilver ores in the Terlingua, Texas. *Econ. Geol.* Vol. 49; p. 175–197.
- Tunnel, G. 1964: Chemical processes in the formation of mercury ores etc. *Geochem. et Cosm. Acta.* Vol. 28; p. 1019–1037.
- Vasilyev, V. I. et al. 1969: A new mercury-bearing species of sphalerite. *Dokl. Acad. Sci. USSR. Earth Sci. Sect.* (137); p. 137–139.
- White, D. S. 1967: Mercury and base metal deposits etc. *Geochem. Hydr. Ore Dep.* (H. L. Barnes), New York, p. 575–631.
- Kiss, J. 1975: Crystallochemical and metallogenetic investigation and evaluation of hydrothermal crystal phase model experiments (25° to 300 °C). *Acta Geol. Ac. Scient. Hung. Tomus* 19 (3–4), pp. 265–274.